Hawaii National Marine Renewable Energy Center (HINMREC)

U.S. Department of Energy Award Number: DE-FG36-08GO18180

Task 6: Supporting Studies

OTEC Heat Exchanger Program: 2013 Progress Reports

Prepared by:
Makai Ocean Engineering

Prepared for:
Hawaii Natural Energy Institute, University of Hawaii

2012 - 2013

HNEI
Hawaiʻi Natural Energy Institute
University of Hawaiʻi at Mānoa

OTEC HEAT EXCHANGER PROGRAM

PROGRESS REPORT #1

Prepared For

HAWAII NATIONAL MARINE RENEWABLE ENERGY CENTER

LUIS VEGA

1680 East West Road, POST 112A

Honolulu, HI, 96822

USA

Prepared By

MAKAI OCEAN ENGINEERING

PO Box 1206, Kailua, Hawaii 96734

May, 2012

SUMMARY

A computer algorithm to automatically detect anomalies in time-lapse images of a corroding aluminum sample was developed. The purpose of this algorithm is to identify possible pit initiation sites to be imaged with a high resolution microscope and to quantify pitting corrosion. The algorithm was verified by testing three different aluminum samples in an existing corrosion imaging apparatus. To image a 36” x 2.5” aluminum sample one time at 20x magnification, 2,576 overlapping photographs were taken. A computer algorithm was developed to stitch these 2,576 images into larger images. To detect anomalies in the time-lapse images, we looked at changes in the pixel intensity values over time. Local pixel darkening or lightening could signal the initiation of pitting corrosion. In Aluminum, a pit site will become visible within a number of days depending on the alloy. To detect these rapidly developing pit sites, the algorithm compares the current day’s image with the image taken several days prior. Any group of pixels that changed in intensity greater than the threshold between those days was recorded as a point of interest to be re-imaged in high resolution. To quantify pitting corrosion over time, the daily images were compared against the image from day 1. Any group of pixels that changed in intensity greater than the threshold was considered an anomaly and most likely a pit. The total number of anomalies and percentage of the sample area that had anomalies versus time was reported. The computer algorithm was successful and proved to have the sensitivity and accuracy required for detecting pit initiation sites. Suggestions for improvements of the algorithm and imaging apparatus are provided.

1. INTRODUCTION

Aluminum corrodes in two ways: uniform corrosion and localized (pitting) corrosion. Uniform corrosion is a relatively slow reduction in metal distributed across the entire surface in contact with seawater, much like one sees on a rusting steel plate exposed to a mild marine environment. Pitting corrosion, in contrast, is an unpredictable, sudden and rapid attack of the metal at a single point on its surface. Pitting corrosion essentially 'drills' a hole in the metal at a rate of up to .002" per day. If the pit passes through the 1/8 inch wall of an OTEC heat exchanger, it would be a catastrophic failure. Our objective in this study is to develop a new technique for measuring pitting growth rates in order to better understand the differences between various alloys and manufacturing processes. Makai has developed several ideas for accurately measuring the growth of pits in situ, which will allow us to take multiple measurements of a single sample without removing it from the test rack. In addition, Makai wants to automate the process in order to reduce human error and allow for a much larger test. For example, counting individual microscopic pits manually is a very tedious process which is better suited to a computer. The initial method which Makai wants to implement and test is photographic imaging. A corrosion test apparatus including a microscope camera mounted on a motorized stage has been recently developed by Makai to collect high resolution digital photographs of the surfaces of corrosion samples. The images of the aluminum samples submerged in seawater are taken through a clear acrylic window. Two cameras are used in this setup. A typical wide field camera images an area of about 0.2 in^2 (0.5" x 0.4" field of view), while a narrow field camera images an area of about 0.001 in^2 (0.04" x 0.03" field of view). Multiple wide field images are taken in a grid pattern and stitched together to create one image of the entire surface. This process is repeated at regular intervals depending on the alloy and exposure time (once per day initially, then once per week after a year of exposure, for example). Each time an image set is acquired, it can be used as a comparison with the previous image set. Makai is developing an algorithm which detects changes automatically. The changes we are looking for are pit initiation sites. When an anomaly is detected, the date and exposure time will be logged, and the narrow field camera will begin to take images each day at this location to obtain a higher resolution image for analysis. This image set will allow us to determine if the anomaly is a pit, and if so estimate the dimensions of the pit at the surface. Over time, we hope to be able to characterize the pitting in aluminum alloys based on initiation times and pit diameters.

2. METHODS

2.1. IMAGE CAPTURING

The aluminum samples in this study were photographed once a day using an existing corrosion imaging apparatus. The photographs were taken using a 2 Megapixel Veho Discovery VMS-004 Deluxe USB microscope camera at 20x magnification. The microscope has a built in LED ring around the lens for illumination. To image the 36” x 2.5” aluminum sample one time at 20x magnification, 2,576 overlapping photographs were taken.

2.2. IMAGE STITCHING

A computer algorithm was developed to stitch the 2,576 images into a pyramid structure of larger images. The stitching algorithm takes four inputs: a matrix of BMP input images acquired from the scanning process, a horizontal overlap parameter, a vertical overlap parameter, and a rotation about the center parameter. The extents of each input image are transformed into the destination coordinate system to determine a final image size that will contain all input images. The destination image is allocated and then scanned in row by column order. For each destination pixel, the coordinates are transformed by the inverse matrix of each input image and the image that contains a pixel closest to the center of the input image is then nearest neighbor interpolated into the destination image. Upon creation of the input image, the image can be successively sub-sampled at half-resolutions to provide a level-of-detail pyramid of images for viewing purposes.

2.3. ANOMALY DETECTION

The computer algorithm to automatically detect anomalies in time-lapse images of corroding aluminum samples was developed using National Instruments Labview and Vision Development Module software. For practical reasons only images of the top 1/11th sections of the aluminum samples were used to test the anomaly detection algorithm. These images are stitched together from 234 images. The stitched images had to be pre-processed prior to the anomaly detection. The color images were first converted to grayscale using a blue color plane extraction. Since the background was still visible in the stitched image, rectangular shape detection was used to identify the aluminum sample and crop the images.

To detect anomalies in the time-lapse images, we looked at changes in the pixel intensity values over time. Local pixel darkening or lightening could signal the initiation of pitting corrosion. In order to accurately compare the intensity values of two images, they must be carefully aligned. Alignment was achieved using perspective, angular, and scale correction. Once the images are aligned, a histogram matching normalization was used to identify bright anomalies within a defined threshold. The intensity threshold was set above the standard deviation of intensity for the whole sample. This threshold was chosen so as not to detect average image intensity fluctuations due to sample darkening or camera and alignment inconsistencies. The intensity threshold used in this study was +30 intensity value in an 8-bit image.

In Aluminum, a pit site will become visible within a number of days depending on the alloy. To detect these rapidly developing pit sites, the algorithm compares the current day’s image with the image taken several days prior. Any group of pixels that changed in intensity greater than the threshold between those days is analyzed. In order to avoid false positives, areas with less than eight surrounding pixels are disregarded. Surrounding pixels of eight or more that are touching are grouped together and considered one anomaly. These areas are recorded as points of interest to be re-imaged in high resolution. To quantify pitting corrosion over time, the daily images were compared against the image from day 1. The total number of anomalies and percentage of the sample area that has anomalies versus time was reported.

3. RESULTS

3.1. ALUMINUM ALLOY PITTING RESULTS

The uncoated aluminum alloy 2024 sample developed the most pits. The algorithm was able to identify the majority of these pits by the white corrosion product that was produced. The number of pits detected increased rapidly during the first three days and then began to slowly decrease as shown in Figure 3-1. The relative pitted area increased rapidly during the first three days and then continued to increase at decreasing rate as shown in Figure 3-2.

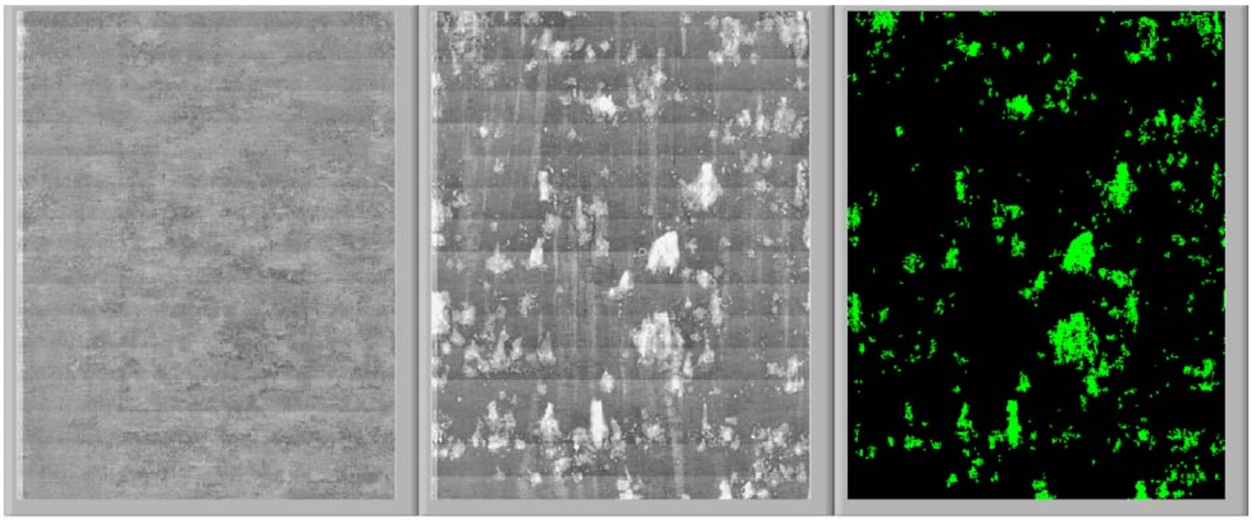

(a) (b) (c)

Figure 3-3: (a) Sample area of Alloy 2024 at day 1. (b) Alloy 2024 at day 26. (c) Detected pitted area shown in green

The aluminum alloy 2024 sample coated with Siloxel developed very few pits. The algorithm detected several anomalies. Upon visual inspection, it was discovered that the majority of these anomalies where not pit sites but just color variations in the metal. Some of the anomalies were due to misalignment in the image stitching. The non-pitted anomalies were removed and pitted areas are shown in the Figure 3-2 below. The two clearly visible pits grew very slowly in size over the course of 25 days.

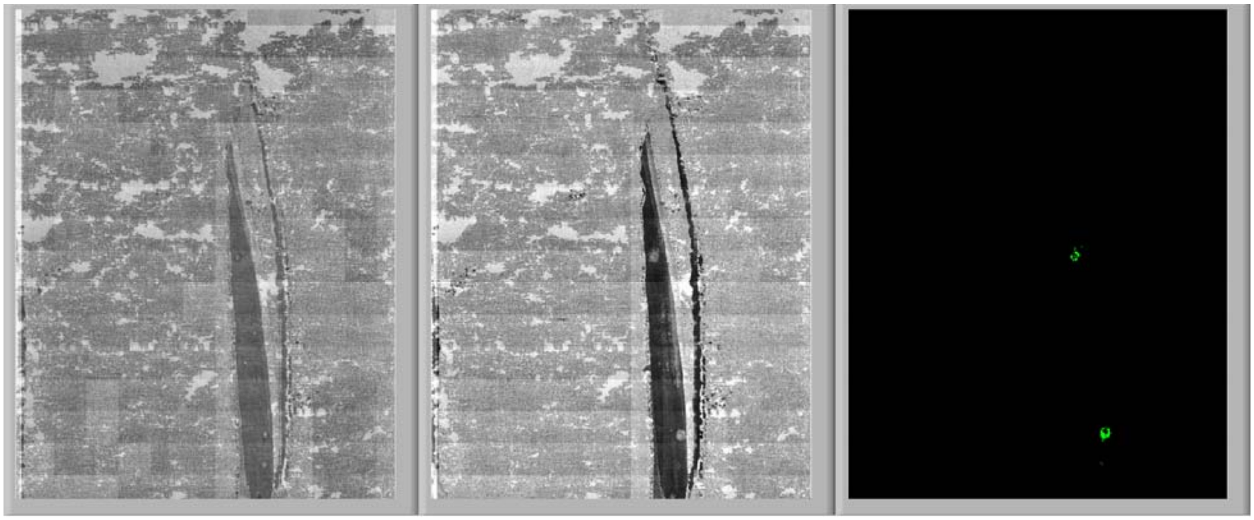

(a) **(b)** **(c)**

Figure 3-4: (a) Sample area of alloy 2024 coated with Siloxel at day 1. (b) Alloy 2024 coated with Siloxel at day 26. (c) Pitted area manually identified in green

The aluminum alloy 3003 sample did not develop any visible pits. The algorithm detected several anomalies where the color changed significantly over the course of 25 days. These anomalies did not appear to be pits.

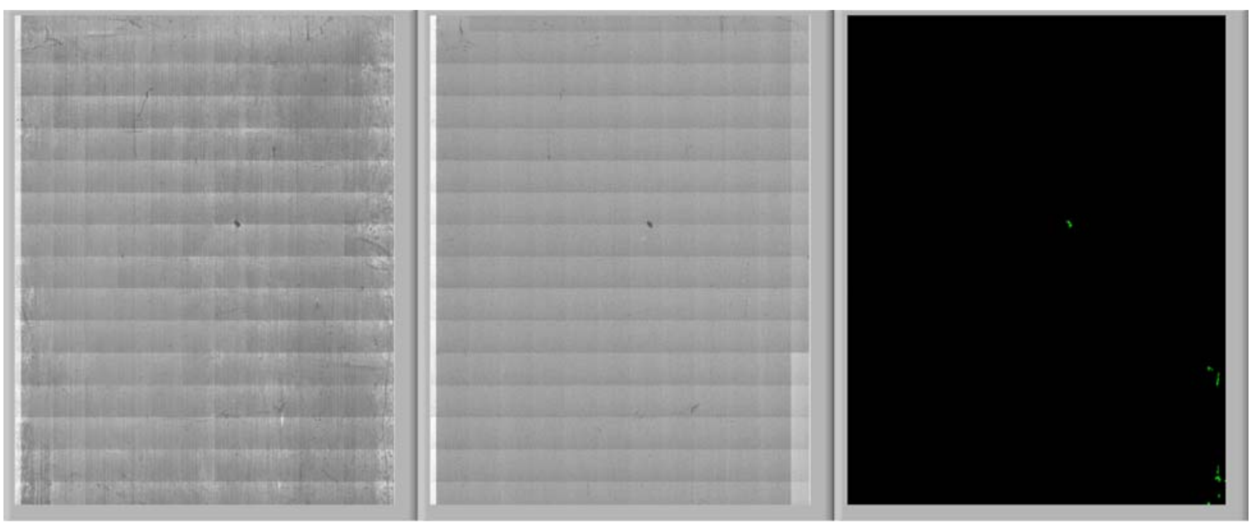

(a) **(b)** **(c)**

Figure 3-5: (a) Sample area of Alloy 3003 at day 1. (b) Alloy 2024 at day 26. (c) Anomalies detected are shown in green

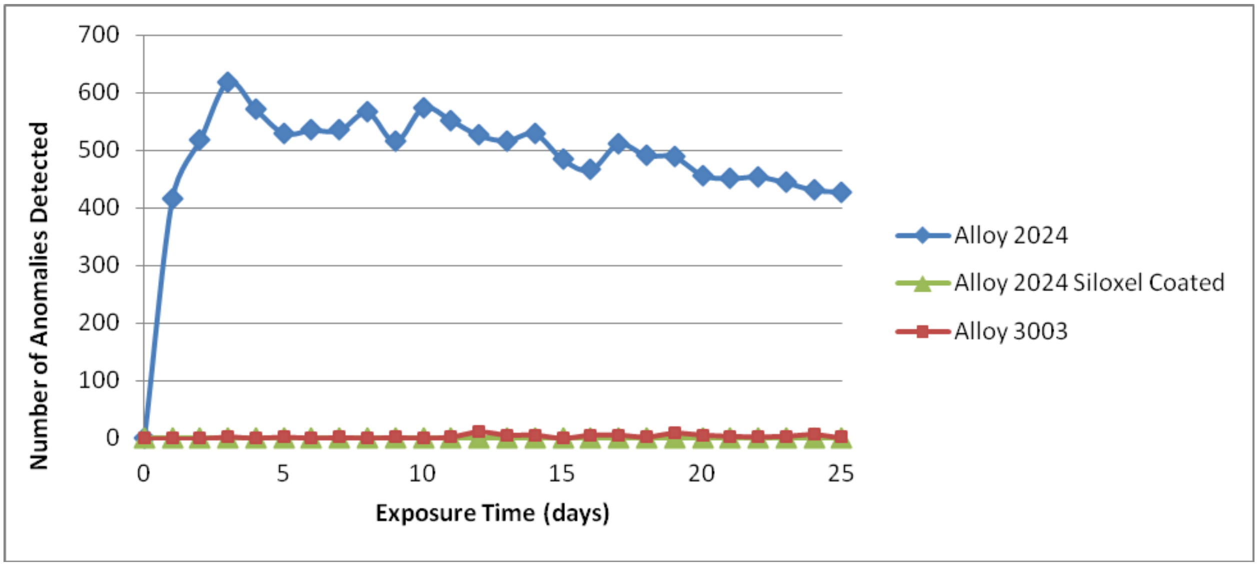

Figure 3-6: Number of anomalies detected for the three different aluminum samples

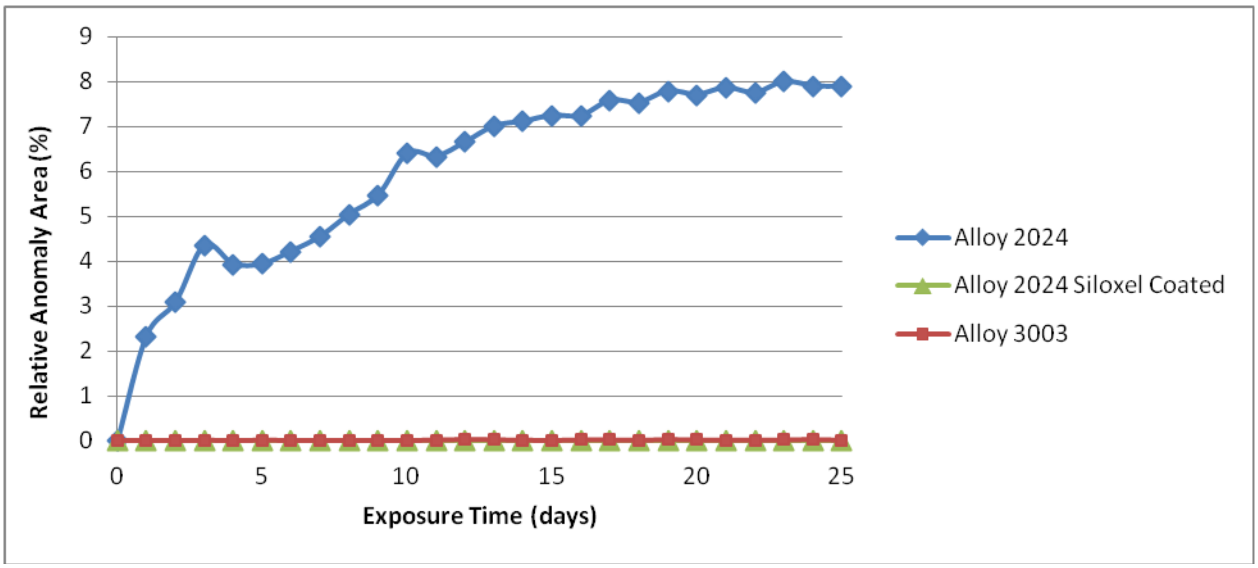

Figure 3-7: Relative anomaly area (%) for the three aluminum samples

4. CONCLUSIONS AND DISCUSSION

4.1. ALGORITHM EFFECTIVNES

The algorithm was successful in detecting anomalies in the sample metal surfaces. The high sensitivity of the algorithm enabled early anomaly detection so that pit initiation and development could be imaged in high resolution. Although not all anomalies become pits, it is important to begin imaging the anomalies in high resolution as soon as possible to capture the potential initiation of pitting corrosion.

4.1.1. Sensitivity

The algorithm is capable of a very high sensitivity of 0.4% changes in intensity. In this study the sensitivity of the algorithm was set to 8.5%, limited by the imaging intervals and the consistency of the imagery. The important consistency parameters were white balance and brightness. The algorithm has enough sensitivity to detect pit initiation sites, however more consistent imagery is required.

4.1.2. Accuracy

The algorithm is capable of detecting anomalies down to 1 pixel in size, however looking for anomalies of 8 surrounding pixels or more removes the majority of false positives. The accuracy and resolution of the algorithm’s detection of anomalies is limited by the alignment accuracy of the imagery. Variations in the alignment of images from day to day can create false anomaly detections. In order to maintain accuracy of the algorithm, the pixel resolution has to match the allowed alignment variation. Since the alignment variation maximum was 5 pixels, the images had to be sub-sampled to reduce the resolution. The imagery used in the study alignment was sufficient for detecting anomalies that are 1 mm or greater in size. The algorithm can detect much smaller anomalies, however it requires better imagery.

4.2. SUGGESTIONS FOR IMPROVEMENT

4.2.1. Sensitivity

- The aluminum samples undergo color changes during exposure in the sea water. In order to increase the sensitivity of the pit detection algorithm, this color change should be investigated further and compensated for in the algorithm.

- Consistency of imagery is the key to the pit detection sensitivity. Camera attributes such as white balance, exposure, brightness and contrast should remain constant for all photographs. Images should be taken at precise time intervals.

- When the ceiling lights are on in the room, it affects the brightness of the images and disrupts the image consistency. Imaging should either take place at night, or a cover should be installed over the cameras to isolate the sample area be photographed.

4.2.2. Accuracy

In order to increase resolution and detect smaller pits, image alignment from stitching needs to be improved. The stitching accuracy can be increased by improving the stitching algorithm and improving the mechanical imaging apparatus.

- The current stitching algorithm applies the same rotation and overlap parameter to each image. Any inaccuracies in mechanical positioning of the camera will results in misaligned stitching. The stitching algorithm can be improved by co-registering each image independently, applying a different rotation and overlap to each image. Ideally, if the stitching algorithm can connect images pixel-for-pixel, the resolution of the anomaly detection algorithm could be maintained closest to the raw image resolution.

- The current imaging apparatus can be improved by using more precise mechanical components and with the addition of position encoders. Using more precise gears or lead screws would help to reduce hysteresis in positioning. Linear encoders would provide very accurate position information for each image taken.

OTEC HEAT EXCHANGER PROGRAM

PROGRESS REPORT #2

Prepared For

HAWAII NATIONAL MARINE RENEWABLE ENERGY CENTER

LUIS VEGA

1680 East West Road, POST 112A

Honolulu, HI, 96822

USA

Prepared By

MAKAI OCEAN ENGINEERING

PO Box 1206, Kailua, Hawaii 96734

July, 2012

SUMMARY

A test apparatus for collecting ultrasonic thickness measurements of aluminum samples was developed. The purpose of this apparatus is to identify and monitor pit sites and to quantify pitting corrosion. The apparatus was verified by measuring a reference plate with the ultrasonic equipment and comparing it with profilometry data. The resolution of the ultrasonic sensor was such that the smallest hole detectable was 0.006 inches diameter by 0.018 inches deep. The ultrasonic apparatus was successful in detecting shallow holes, and proved to have the sensitivity and accuracy required for detecting corrosion pit sites. Several methods for improving both the resolution and accuracy of the apparatus are discussed.

1. INTRODUCTION

Aluminum corrodes in two ways: uniform corrosion and localized (pitting) corrosion. Uniform corrosion is a relatively slow reduction in metal distributed across the entire surface in contact with seawater, much like one sees on a rusting steel plate exposed to a mild marine environment. Pitting corrosion, in contrast, is an unpredictable, sudden and rapid attack of the metal at a single point on its surface. Pitting corrosion essentially 'drills' a hole in the metal at a rate of up to .002" per day. If the pit passes through the 1/8 inches wall of an OTEC heat exchanger, it would be a catastrophic failure. Our objective in this study is to develop a new technique for measuring pitting growth rates in order to better understand the differences between various alloys and manufacturing processes. Makai has developed several ideas for accurately measuring the growth of pits in situ, which will allow us to take multiple measurements of a single sample without removing it from the test rack. In addition, Makai wants to automate the process in order to reduce human error and allow for a much larger test. For example, counting individual microscopic pits manually is a very tedious process which is better suited to a computer. The initial method which Makai implemented and tested was photographic imaging. The second method which Makai wants to implement and test is ultrasonic imaging. Corrosion mapping, which is based on ultrasonic technology, is one technique used by industry to monitor wall thickness in piping or tanks. This technique utilizes the speed of sound travelling through a metal wall to determine its thickness. Typically, it is used as a safety precaution when hazardous materials are contained inside, especially if the pipe or tank is under pressure. Makai has confirmed this technique can be used to map the pits that develop in our aluminum samples. The benefit of this technology in our application is that we can monitor the growth of these pits, without removing the sample from the test. Once a pit is detected using the photographic imaging technique, the region will be scanned using an ultrasonic transducer. The change in thickness will be mapped according to its X-Y position using a motorized stage, and co-registered with the image data. Ultrasonic scans will be repeated on a daily basis to monitor changes. The main goal of the ultrasonic method is to determine the rate of pit growth through the wall, without removing the sample from the test rack. This information will be used to calculate the expected life of a heat exchanger.

2. METHODS

2.1. X-Y STAGE

The ultrasonic transducer and profilometer used in this study were individually mounted on a motorized X-Y stage. The X-Y stage was powered by stepper motors, capable of moving at speeds up to 200mm/second. Encoders mounted on each axis allowed position to be recorded with a resolution of 5 micron. The test pieces to be scanned are secured to the bottom plate of the X-Y stage.

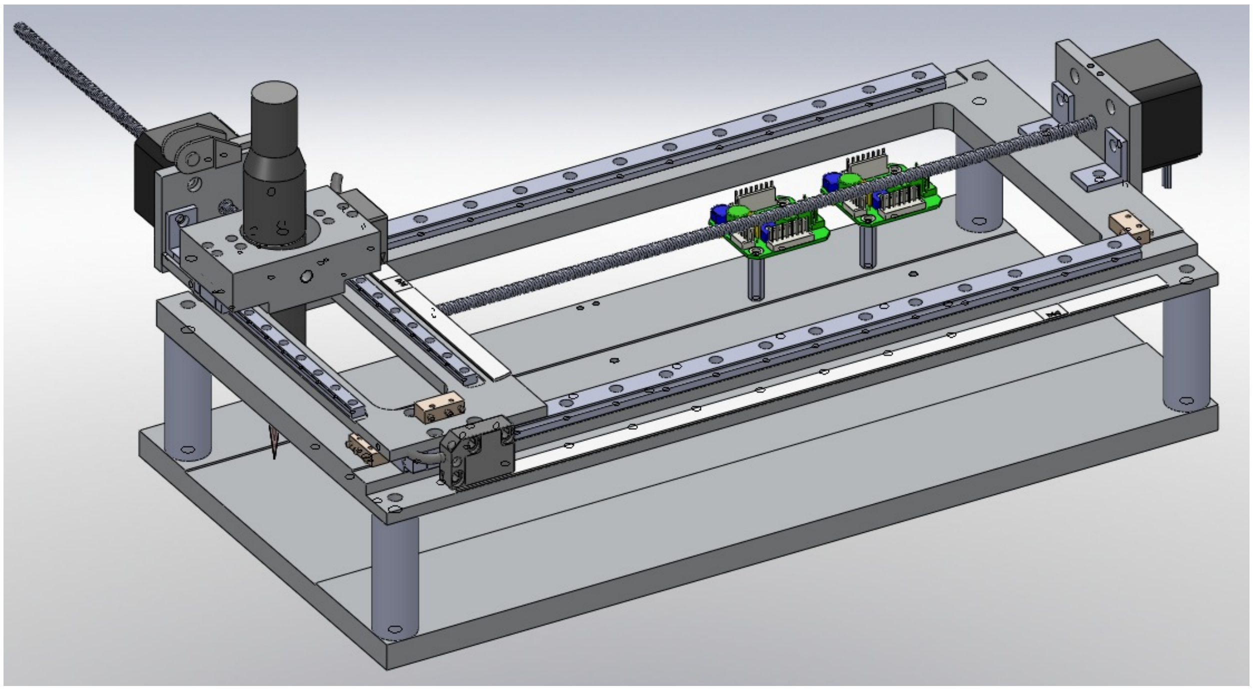

Figure 2-1: Motorized X-Y stage for ultrasonic and profilometer scanning.

2.2. CALIBRATION BLOCK

A custom reference plate was made that contained an array of small holes, varying in both depth and diameter. This aluminum calibration block was designed to test the sensitivity of the ultrasonic equipment. It contains three holes of each of the following diameters (in inches): 0.006, 0.009, 0.013, 0.016, 0.028 with varying depths as shown in Figure 2-2 and in Figure 2-3. On the opposite side of where the holes were drilled, a 0.16 inches deep pocket was made to contain the water used as an ultrasonic fluid. The engineering drawing of the calibration block can be seen in Figure 2-2. Because of manufacturing inaccuracies, the holes and block thickness had some variation. The profilometer was used to measure the actual hole diameters and depths of the manufactured calibration block.

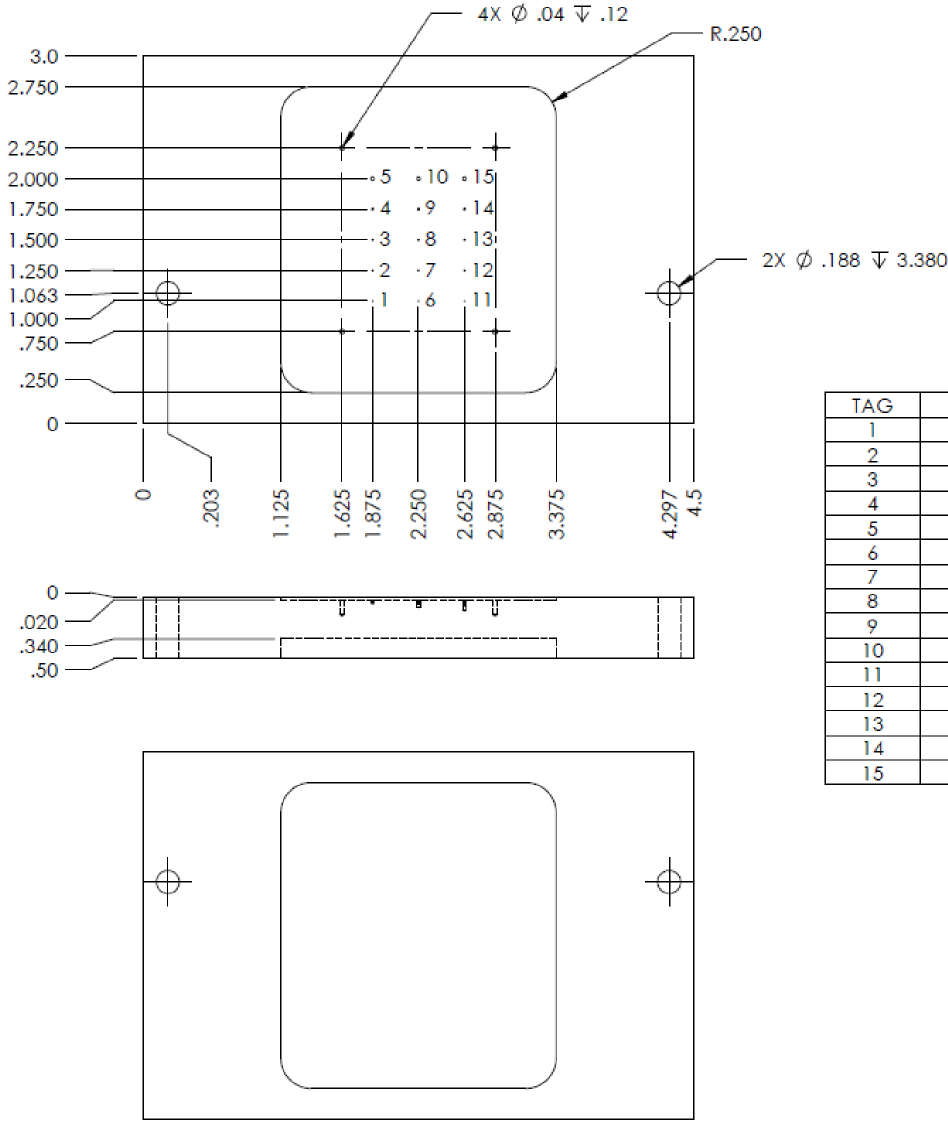

TAG	SIZE
1	⌀ .006 ↧ .006
2	⌀ .009 ↧ .009
3	⌀ .013 ↧ .013
4	⌀ .016 ↧ .016
5	⌀ .028 ↧ .028
6	⌀ .006 ↧ .012
7	⌀ .009 ↧ .018
8	⌀ .013 ↧ .025
9	⌀ .016 ↧ .032
10	⌀ .028 ↧ .056
11	⌀ .006 ↧ .020
12	⌀ .009 ↧ .027
13	⌀ .013 ↧ .039
14	⌀ .016 ↧ .048
15	⌀ .028 ↧ .084

Figure 2-2: Engineering drawing for the ultrasonic calibration block including hole dimensions.

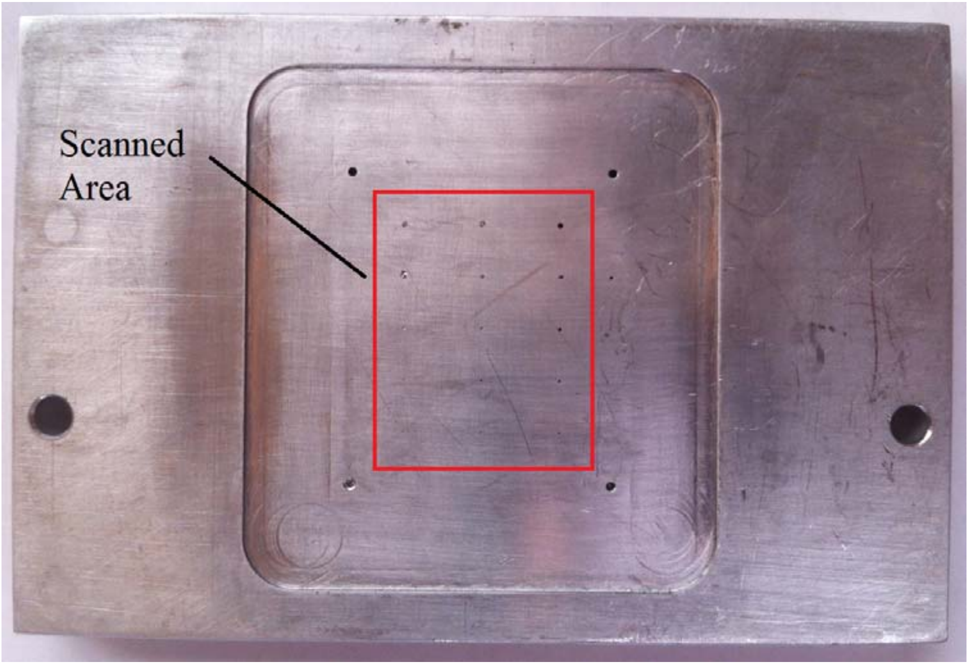

Figure 2-3: Photograph of ultrasonic calibration block with the profilometer and ultrasonic scan area highlighted by the red rectangle.

2.3. ULTRASONIC APPARATUS

The ultrasonic apparatus consists of a transducer, a transducer holder, a spring, and cable to a handheld thickness gauge instrument. The thickness gauge is connected to the computer via USB and transmits the thickness data at frequency 100HZ. The transducer is a high resolution delay line type with a 0.188 inches element and operates at a frequency of 15 MHz. The ultrasonic assembly was mounted vertically on the X-Y stage. The transducer's face is pressed against the bottom of the calibration block pocket with pressure from the spring. The pocked is filled with water. The calibration block was scanned with a resolution of 0.001" x 0.001" and 0.002" x 0.002". The measured thickness was plotted with software provided with the ultrasonic equipment.

2.4. PROFILOMETRY APPARATUS

An optical profilometer pen was mounted vertically on the X-Y stage. The profilometer has an accuracy of +/- 8 µm in the z-direction (perpendicular to the scan plane) and +/- 5 µm in the x and y direction (within the scan plane). The profilometer was used to scan the calibration block and verify the diameters and depths of each individual hole. The profilometer is the most precise and accurate sensor available to us for hole size measurement. For this reason the profilometry scan data was used as the "actual size" reference in which to evaluate the accuracy of ultrasonic scan data.

3. RESULTS

3.1. PROFILOMETRY SCAN

The three dimensional surface of calibration block scanned using the optical profilometer is shown in Figure 3-1. All fifteen of the holes tagged 1-15 were visible in the profilometer data.

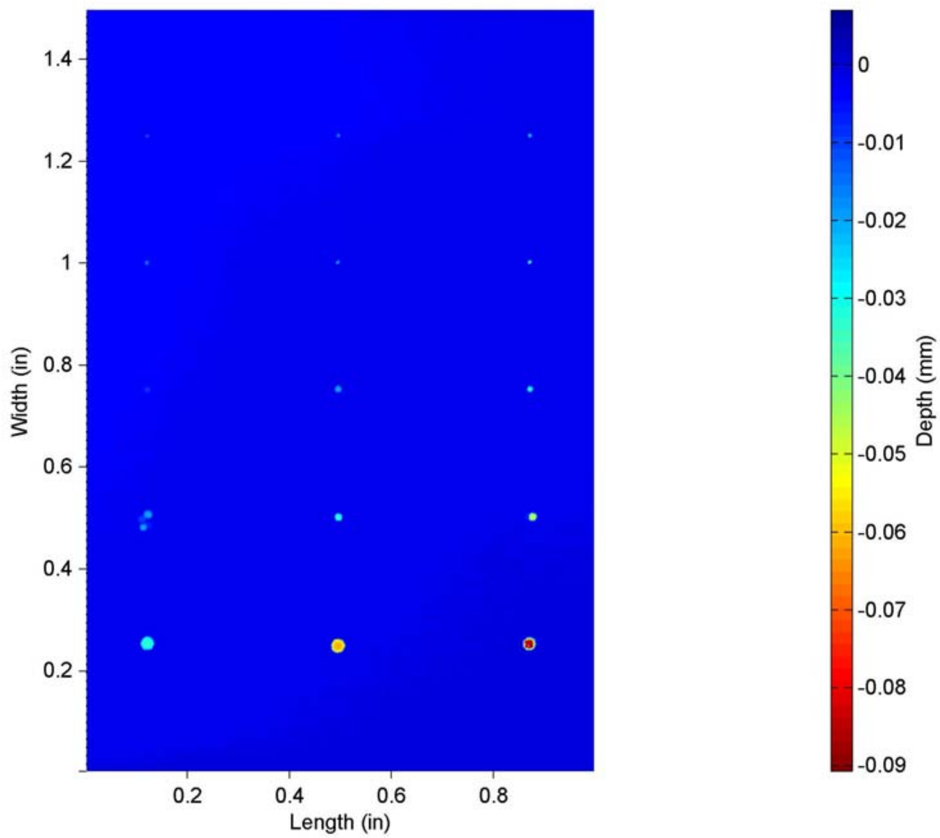

Figure 3-1: Top view of the profilometer scan data for the top surface of the ultrasonic calibration block

The optical profilometer scan of the calibration block revealed a small difference between the specified hole dimensions in the design drawing, and the measured hole dimensions of the manufactured part. The difference in dimensions between the drawing specifications and the profilometry data is called the dimension error and is shown in Table 3-1.

Table 3-1: Specified hole dimensions, measured profilometer hole dimensions and the dimension error for holes in the ultrasonic calibration block.

HOLE	DESIGN SPECIFIED SIZE (IN)		PROFILOMETER MEASURED SIZE (IN)		DIMENSION ERROR (IN)	
TAG	DIAMETER	DEPTH	DIAMETER	DEPTH	DIAMETER	DEPTH
1	0.006	0.006	0.006	0.009	0.000	0.003
2	0.009	0.009	0.009	0.013	0.000	0.004
3	0.013	0.013	0.013	0.011	0.000	0.002
4	0.016	0.016	0.015	0.018	0.001	0.002
5	0.028	0.028	0.022	0.031	0.006	0.003
6	0.006	0.012	0.007	0.014	0.001	0.002
7	0.009	0.018	0.009	0.024	0.000	0.006
8	0.013	0.025	0.013	0.019	0.000	0.006
9	0.016	0.032	0.012	0.032	0.004	0.000
10	0.028	0.056	0.025	0.059	0.003	0.003
11	0.006	0.020	0.006	0.021	0.000	0.001
12	0.009	0.027	0.009	0.023	0.000	0.004
13	0.013	0.039	0.013	0.033	0.000	0.006
14	0.016	0.048	0.013	0.048	0.003	0.000
15	0.028	0.084	0.020	0.087	0.008	0.003
		AVERAGE DIMENSION ERROR (IN)			0.002	0.003
		MAXIMUM DIMENSION ERROR (IN)			0.008	0.006

Previous verification testing on the accuracy of the profilometer reveals that the profilometer is accurate to within the specified value. When comparing the measured values of the holes with the design specification, the average hole diameter error was 0.002 inches and the average hole depth error was 0.003 inches. The maximum hole diameter error was 0.008 inches and the maximum hole depth error was 0.006 inches. These errors are expected given the manufacturing process used during fabrication.

3.2. ULTRASONIC SCANS

3.2.1. <u>0.001” x 0.001” Resolution Scan</u>

The three dimensional surface of the calibration block scanned using the ultrasonic thickness sensor with a resolution of 0.001 x 0.001 inches is shown in Figure 3-2. Ten out of the fifteen holes were identified in the ultrasonic scan. The holes tagged 5 and 7-15 were identified while holes 1-4 and 6 were not identified.

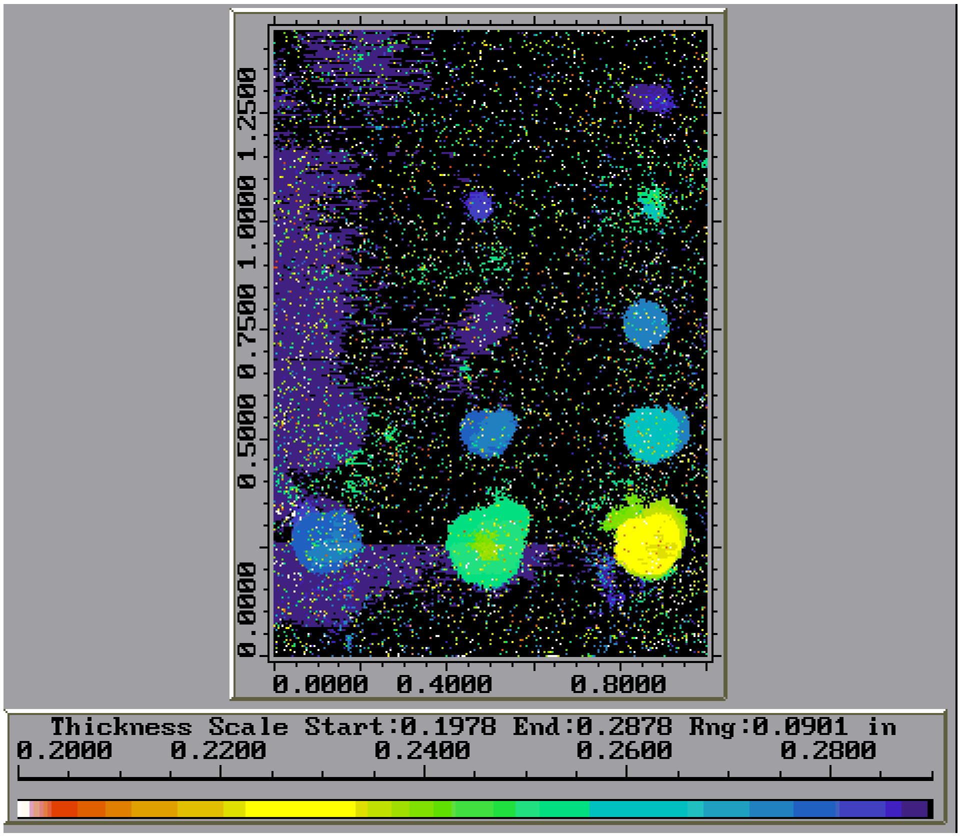

Figure 3-2: Top view of the 0.001"x0.001" resolution ultrasonic scan of the top surface of the ultrasonic calibration block

The ultrasonic thickness sensor was not able to measure holes with a depth of less than 0.018 inches. The ultrasonic thickness sensor was able to measure the entire range of holes tested between 0.006 and 0.028 inches in diameter.

3.2.2. <u>0.002" x 0.002" Resolution Scan</u>

The three dimensional surface of the calibration block scanned using the ultrasonic thickness sensor with a resolution of 0.002 x 0.002 inches is shown in Figure 3-3. Eight out of the fifteen holes were identified in the ultrasonic scan. The holes tagged 5, 7, 9, 10, and 12-15 were identified. Holes 1-4, 6, 8 and 11 were not identified.

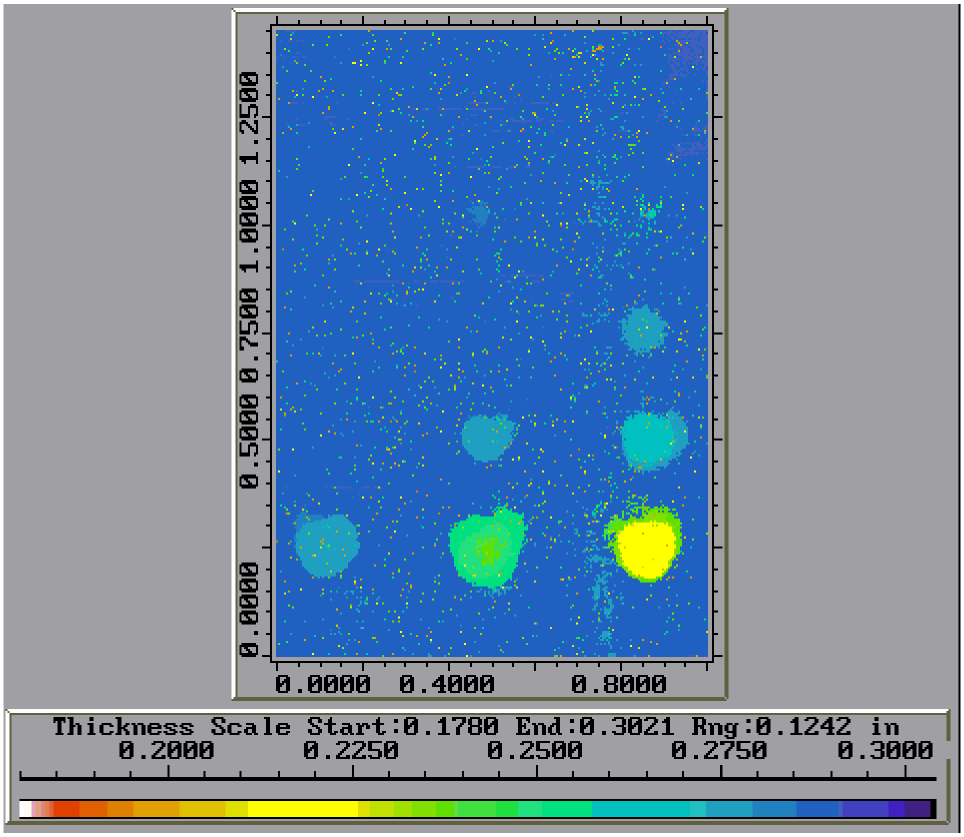

Figure 3-3: Top view of the 0.002"x0.002" resolution ultrasonic scan of the top surface of the ultrasonic calibration block

The ultrasonic thickness sensor was not able to measure holes with a depth of less than 0.021 inches. The ultrasonic thickness sensor was able to measure the entire range of holes tested between 0.009 and 0.028 inches in diameter.

3.2.3. Repeatability test

The higher resolution 0.001" x 0.001" ultrasonic scan detected more holes than the lower resolution 0.002" x 0.002" scan. The hole depth measurements of both scans and the repeatability error is shown in Table 3-2. The average repeatability error of depth measurement between the two scans was 0.001 inches. The maximum repeatability error was 0.003 inches.

Table 3-2: Measured dimensions and repeatability error of the holes in the ultrasonic calibration block.

HOLE	0.001” x 0.001” SCAN MEASURED SIZE (IN)	0.002” x 0.002” SCAN MEASURED SIZE (IN)	REPEATABILITY ERROR (IN)
TAG	DEPTH	DEPTH	DEPTH
1	0	0	0
2	0	0	0
3	0	0	0
4	0	0	0
5	0.014	0.015	0.001
6	0	0	0
7	0.006	0.006	0
8	0.002	0	0.002
9	0.015	0.015	0
10	0.052	0.050	0.002
11	0.003	0	0.003
12	0.035	0.035	0
13	0.016	0.015	0.001
14	0.028	0.030	0.002
15	0.068	0.070	0.002
AVERAGE REPEATABILITY ERROR (IN)			0.001
MAXIMUM REPEATABILITY ERROR (IN)			0.003

3.3. HOLE SIZE COMPARISON

Measured hole depths between the reference profilometer scan and the higher resolution 0.001” x 0.001” ultrasonic scan are compared. The depth of each hole recorded in the profilometer and ultrasonic scans is listed in Table 3-3. The measurement error of the ultrasonic scan based on the profilometer data as a reference is also listed in Table 3-3. The average ultrasonic depth measurement error was 0.014 inches, with a maximum of 0.020 inches. There was only one hole measurement error with a negative value. The specified and measured depths of each hole is plotted in Figure 3-4.

Table 3-3: Design specified size, profilometer measured size, ultrasonic measured size and ultrasonic depth measurement error of each hole in the ultrasonic calibration block.

HOLE	DESIGN SPECIFIED SIZE (IN)		PROFILOMETER MEASURED SIZE (IN)		ULTRASONIC MEASURED SIZE (IN)	ULTRASONIC MEASURMENT ERROR (IN)	ULTRASONIC MEASURMENT ERROR (%)
TAG	DIAMETER	DEPTH	DIAMETER	DEPTH	DEPTH	DEPTH	DEPTH
1	0.006	0.006	0.006	0.009	0	0.009	100.0
2	0.009	0.009	0.009	0.013	0	0.013	100.0
3	0.013	0.013	0.013	0.011	0	0.011	100.0
4	0.016	0.016	0.015	0.018	0	0.018	100.0
5	0.028	0.028	0.022	0.031	0.014	0.017	54.8
6	0.006	0.012	0.007	0.014	0	0.014	100.0
7	0.009	0.018	0.009	0.024	0.006	0.018	75.0
8	0.013	0.025	0.013	0.019	0.002	0.017	89.5
9	0.016	0.032	0.012	0.032	0.015	0.017	53.1
10	0.028	0.056	0.025	0.059	0.052	0.007	11.9
11	0.006	0.02	0.006	0.021	0.003	0.018	85.7
12	0.009	0.027	0.009	0.023	0.035	-0.012	52.2
13	0.013	0.039	0.013	0.033	0.016	0.017	51.5
14	0.016	0.048	0.013	0.048	0.028	0.02	41.7
15	0.028	0.084	0.02	0.087	0.068	0.019	21.8
AVERAGE ULTRASONIC MEASURMENT ERROR (IN)						0.014	
MAXIMUM ULTRASONIC MEASURMENT ERROR (IN)						0.020	

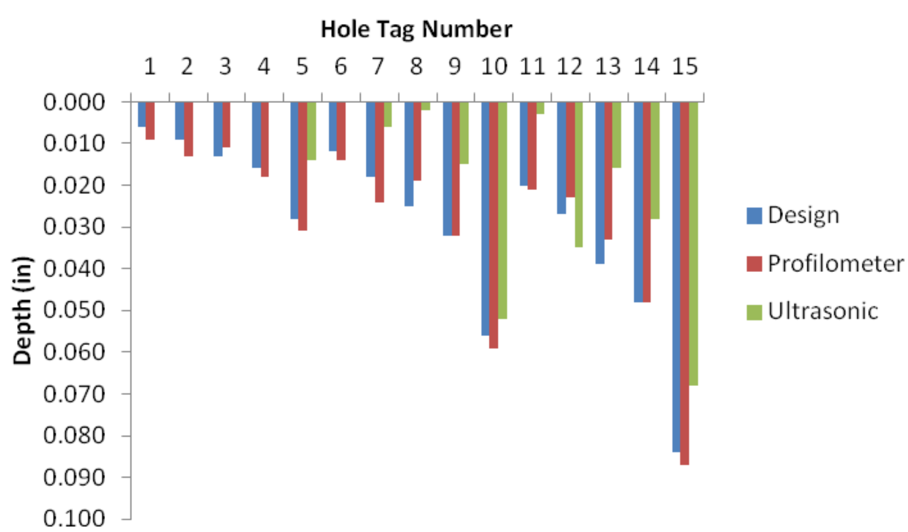

Figure 3-4: Depth of holes 1-15 in the ultrasonic calibration block as specified in the engineering drawing and as measured using profilometer and ultrasonic scans.

The error in the ultrasonic depth measurement relative to the reference profilometer scan is shown in Figure 3-5. The data suggest that the error increases with decreasing hole diameter.

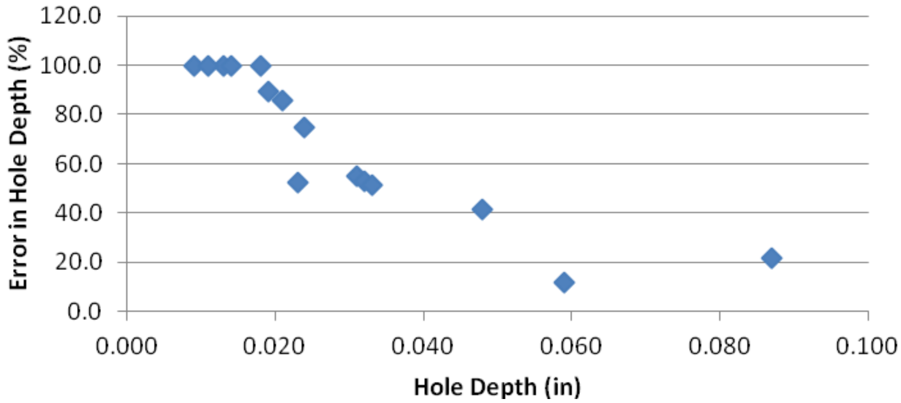

Figure 3-5: Ultrasonic measurement error of hole depth as a function of actual hole depth as measured by the profilometer in the ultrasonic calibration block.

4. CONCLUSIONS AND DISCUSSION

4.1. ULTRASONIC

4.1.1. Repeatability

The ultrasonic thickness sensor scanning at the higher resolution of 0.001 x 0.001 inches was successful in detecting holes with a depth greater than 0.018 inches. The higher resolution ultrasonic scan was able to detect shallower holes than the lower resolution ultrasonic scan. Hence, the scan resolution is an important parameter in the detection of very shallow holes. Comparing the measurements of the holes that were detected, both ultrasonic scans showed very good agreement on hole depth. The maximum repeatability error of holes that were measured by both scans was 0.002 inches. This could be possibly attributed to sensor measurement error. The repeatability test demonstrated that at different scan resolutions, the measurement accuracy is repeatable but detection of shallow hole suffers at lower resolutions.

4.1.2. Resolution

The ultrasonic sensor at a high scan resolution was capable of detecting holes with depths as shallow as 0.018 inches and with diameters as small as 0.006 inches. The ultrasonic sensor manufacturer suggests that we are approaching the technology's capability limit for detecting shallow holes. Further testing at higher scan resolutions and using different ultrasonic transducers would be required to verify the limit of ultrasonic's ability to detect very shallow pits.

4.1.3. Accuracy

The accuracy in determining hole depth is accurate to within 22% for hole depths up to 0.060 inches. Larger than hole depths of 0.060 inches, the measuring accuracy decreases with the hole depth. Above a depth of 0.018 inches, the ultrasonic sensor could not detect holes. The majority of the ultrasonic measurement error values with the exception of one were positive values. The average ultrasonic measurement error was 0.014 inches. This reveals that the ultrasonic measurements were consistently underestimating the depth. With further testing this average error could be better characterized and used as a correction factor in determining actual pit depths from ultrasonic measurements.

4.2. SUGGESTIONS FOR IMPROVEMENT

4.2.1. Repeatability

The repeatability test inadvertently demonstrated that higher resolution scans can detect shallower holes. This result could be explored further by incrementally increasing scan resolution until convergence occurs. This information would allow for the most appropriate resolution to be used given the desired detectable pit depth in future experiments.

4.2.2. Resolution

Since it was demonstrated that increasing the scan resolution increases the pit depth resolution, this technique should be explored to identify the resolution limit of this ultrasonic transducer. Further increasing pit depth resolution would most likely require experimenting with different transducer types.

4.2.3. Accuracy

Further testing would reveal if increasing the scan resolution would increase hole depth accuracy as well as resolution. With enough ultrasonic hole measurement data, statistical methods could be used to calculate a hole depth correction factor.

OTEC HEAT EXCHANGER PROGRAM

PROGRESS REPORT #3

Prepared For

HAWAII NATIONAL MARINE RENEWABLE ENERGY CENTER

LUIS VEGA

1680 East West Road, POST 112A

Honolulu, HI, 96822

USA

Prepared By

MAKAI OCEAN ENGINEERING

PO Box 1206, Kailua, Hawaii 96734

June, 2013

SUMMARY

A test apparatus that integrates time-lapse imaging and ultrasonic thickness measurements of aluminums sample submerged in flowing seawater was designed and built. The purpose of this apparatus is to identify pitting corrosion with camera imagery and subsequently monitor these locations with an ultrasonic thickness sensor in situ. Pitting corrosion will be quantified by measuring the size and depths of pits at regular time intervals with an ultrasonic thickness gage. The apparatus consists of two motorized scanners mounted on either side of an aluminum sample. The camera scanner is mounted on the front of the corrosion rack and images the aluminum sample through the clear acrylic window and the flowing seawater channel. The ultrasonic scanner is mounted on the back of corrosion rack and contacts the back side of the Aluminum sample. A test was conducted to verify that the imaging apparatus and the ultrasonic apparatus worked correctly. The test was successful in demonstrating that the corrosion apparatus functioned correctly and that the imaging and corrosion data could be integrated.

1. INTRODUCTION

Aluminum corrodes in two ways: uniform corrosion and localized (pitting) corrosion. Uniform corrosion is a relatively slow reduction in metal distributed across the entire surface in contact with seawater, much like one sees on a rusting steel plate exposed to a mild marine environment. Pitting corrosion, in contrast, is an unpredictable, sudden and rapid attack of the metal at a single point on its surface. Pitting corrosion essentially 'drills' a hole in the metal at a rate of up to .002" per day. If the pit passes through the 1/8 inches wall of an OTEC heat exchanger, it would be a catastrophic failure. Our objective in this study is to develop a new technique for measuring pitting growth rates in order to better understand the differences between various alloys and manufacturing processes. Makai has developed several ideas for accurately measuring the growth of pits in situ, which will allow us to take multiple measurements of a single sample without removing it from the test rack. In addition, Makai wants to automate the process in order to reduce human error and allow for a much larger test. For example, counting individual microscopic pits manually is a very tedious process which is better suited to a computer. The initial method which Makai implemented and tested was photographic imaging. The second method which Makai wants to implement and test is ultrasonic imaging. Corrosion mapping, which is based on ultrasonic technology, is one technique used by industry to monitor wall thickness in piping or tanks. This technique utilizes the speed of sound travelling through a metal wall to determine its thickness. Typically, it is used as a safety precaution when hazardous materials are contained inside, especially if the pipe or tank is under pressure. Makai has confirmed this technique can be used to map the pits that develop in our aluminum samples. The benefit of this technology in our application is that we can monitor the growth of these pits, without removing the sample from the test. Once a pit is detected using the photographic imaging technique, the region will be scanned using an ultrasonic transducer. The change in thickness will be mapped according to its X-Y position using a motorized stage, and co-registered with the image data. Ultrasonic scans will be repeated on a daily basis to monitor changes. The main goal of the ultrasonic method is to determine the rate of pit growth through the wall, without removing the sample from the test rack. This information will be used to calculate the expected life of a heat exchanger.

2. DESIGN & FABRICATION

2.1. CORROSION RACK

A corrosion rack was designed and built by Makai Ocean Engineering to test 15 flat metal bar samples simultaneously. The corrosion rack's frame measures 1960 mm long by 1380 mm tall and is mounted 580 mm off the ground for easy viewing. There are 15 individual sea water channel slots in the rack; one for each sample. Each slot consisted of a Delrin sea water channel with acrylic glass on the front and the aluminum sample on the back. The clear acrylic glass allows the aluminum sample to be visually monitored for corrosion from the front. A motorized X-Y-Z stage was integrated into the corrosion rack design to provide time lapse imaging of the corrosion samples. The imaging apparatus will be discussed in greater detail in the following section 2.2. The samples designed for this experiment are 1199 x 102 x 9.5 mm machined aluminum plates of various alloys. The plates were mounted to the back of the corrosion rack, allowing the front face to be exposed to flowing sea water. A gasket around the entire edge of the sample's front face seals the sea water channel.

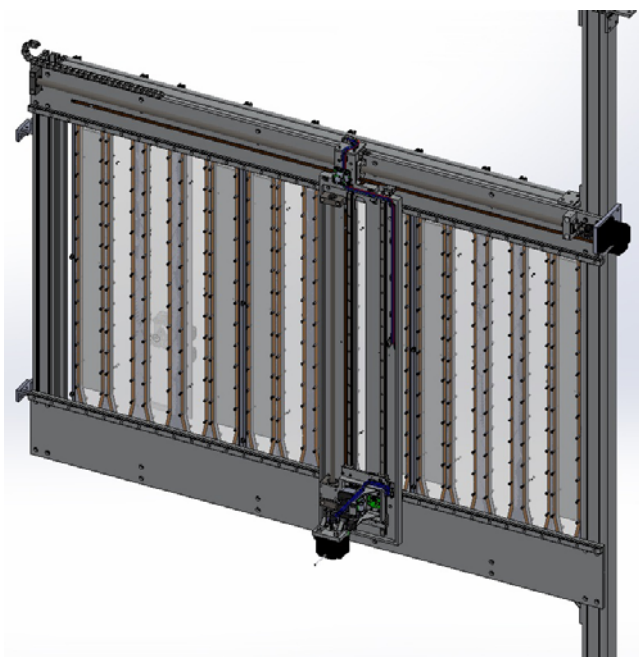

(a)

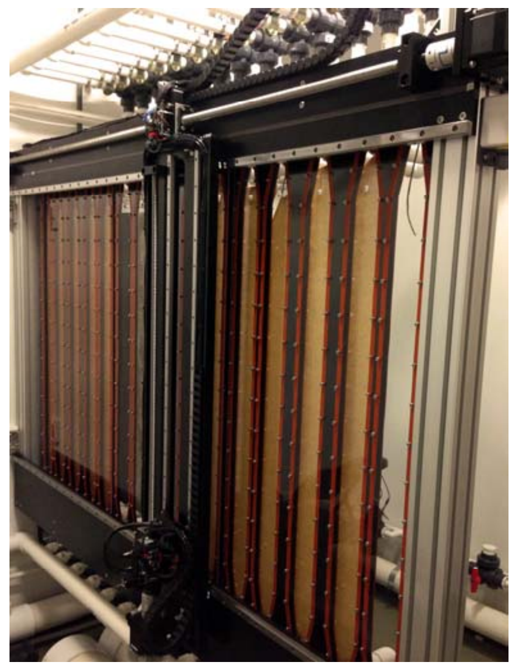

(b)

Figure 2-1: (a) 3-D solid model design of Makai's corrosion rack. (b) Photograph of Makai's corrosion rack fully assembled.

2.2. IMAGING APPARATUS

A custom imaging apparatus consisting of two cameras mounted on a motorized stage was developed. This apparatus collects high resolution digital photographs of aluminum samples submerged in seawater through a clear acrylic window. The cameras are both Edmund Optics-5012C ½" CMOS color GigE machine vision with 5 megapixel resolution. The bottom camera was fitted with a wide field lens and the top with a high magnification lens. The wide field lens is an Edmund Optics Ultra High Resolution 12 mm lens. This lens provides a field of view of 64 mm with an image resolution of 0.04 pixels/micron. The high magnification lens is an Edmund Optics Techspec 6X compact telecentric lens with a 65mm working distance. The high magnification provides a field of view of 1 mm with an image resolution of 2.75 pixels/micron. The X and Y axes are fitted with 0.005 mm resolution encoders to provide accurate image positions. The wide field images are taken in a vertical line pattern and stitched together to create one image of the entire surface daily. These images are analyzed and areas of interest are identified. The areas of interest could be pits or strange features and are imaged with the high magnification camera daily.

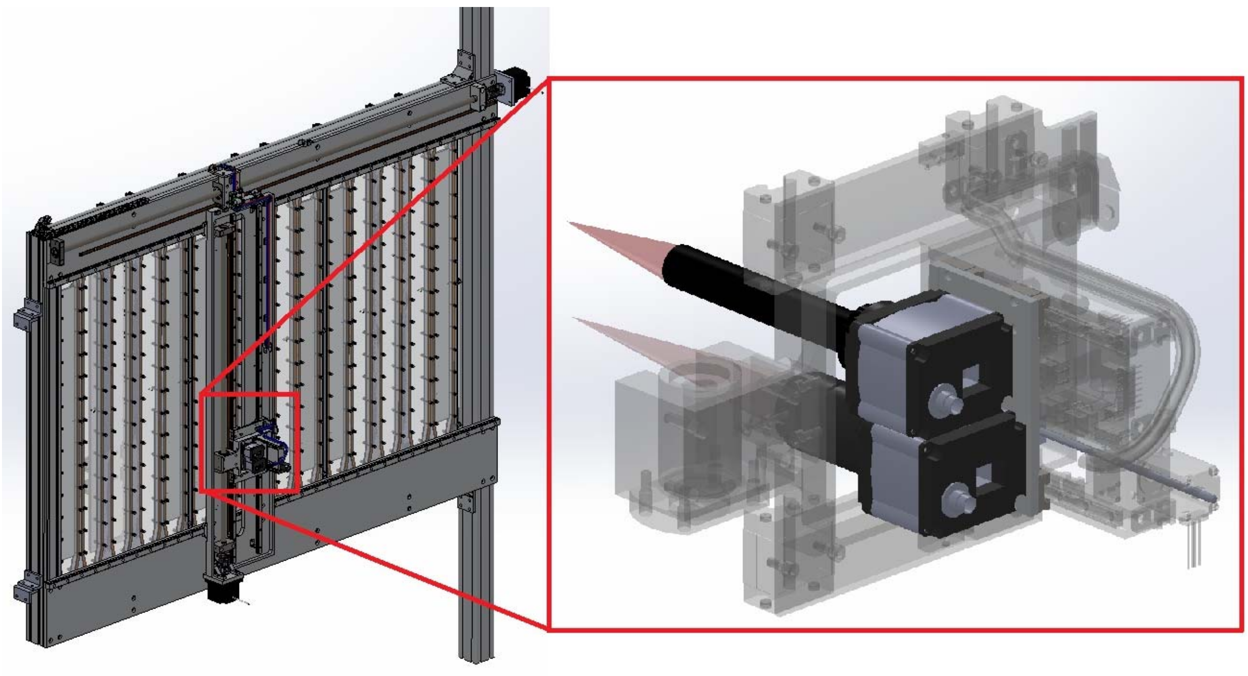

Figure 2-2: 3-D solid model design of Makai's corrosion rack with motorized X-Y-Z stage and imaging apparatus. Zoomed in view shows the Y-stage and Z-stage with the two mounted cameras. The top camera has the long microscope lens attached and the bottom camera has the short wide field of view lens. The transparent red cones protruding from the lenses indicate their respective focal points.

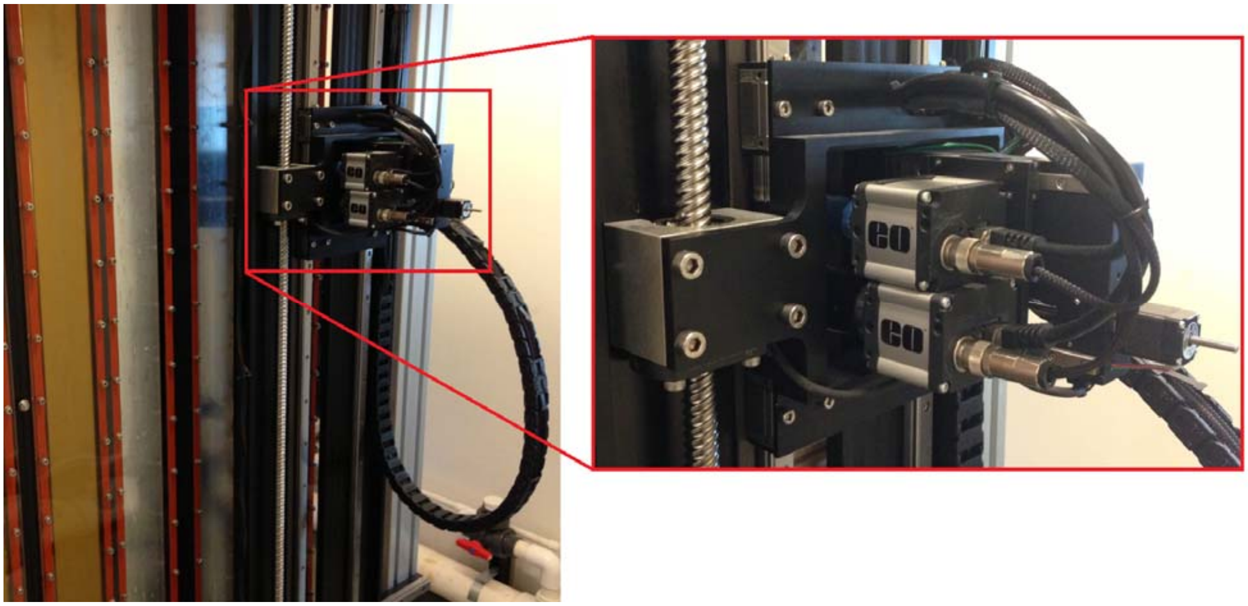

Figure 2-3: Photograph of Makai's corrosion rack with motorized X-Y-Z stage and imaging apparatus. Zoomed in view shows the Y-stage and Z-stage with the two mounted cameras. The top camera has the long microscope lens attached and the bottom camera has the short wide field of view lens.

2.3. PROFILOMETRY APPARATUS

The profilometer apparatus consisted of a profilometer instrument and an optical pen mounted on a motorized X-Y stage. The profilometer instrument was a Nanovea® P9-CCSPRI CCS Prima 1 Channel with a P1-OP12MMD, 10.0mm range and 8.00 μm accuracy (in the z-direction perpendicular to the scan plane) optical pen. The X-Y stage was powered by stepper motors, and position was recorded with 5 μm resolution encoders. The test pieces to be scanned were secured to the bottom plate of the X-Y stage. The profilometer was used to scan the Aluminum corrosion sample before the sea water emersion test was started to verify the diameters and depths of the indexing holes. The profilometer is the most precise and accurate sensor available to us for hole size measurement. For this reason the profilometry scan data was used as the "actual size" reference in which to evaluate the accuracy of ultrasonic scan data.

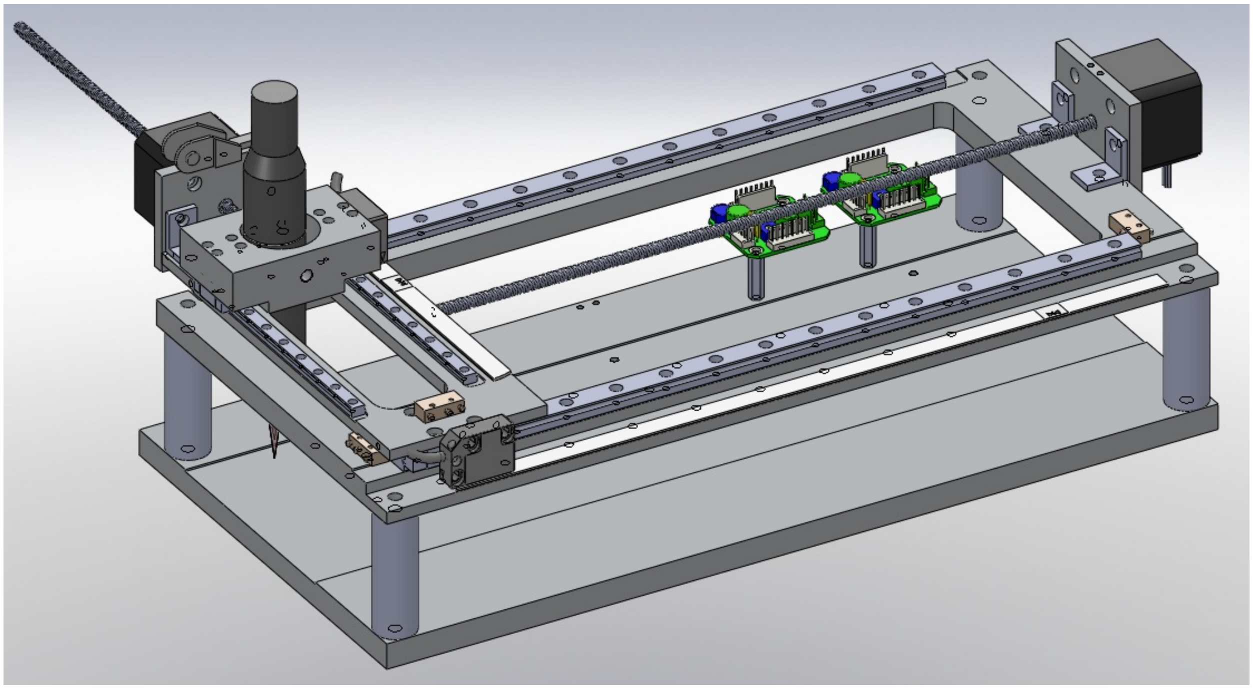

Figure 2-4: 3-D solid model design of Makai's motorized profilometer X-Y stage.

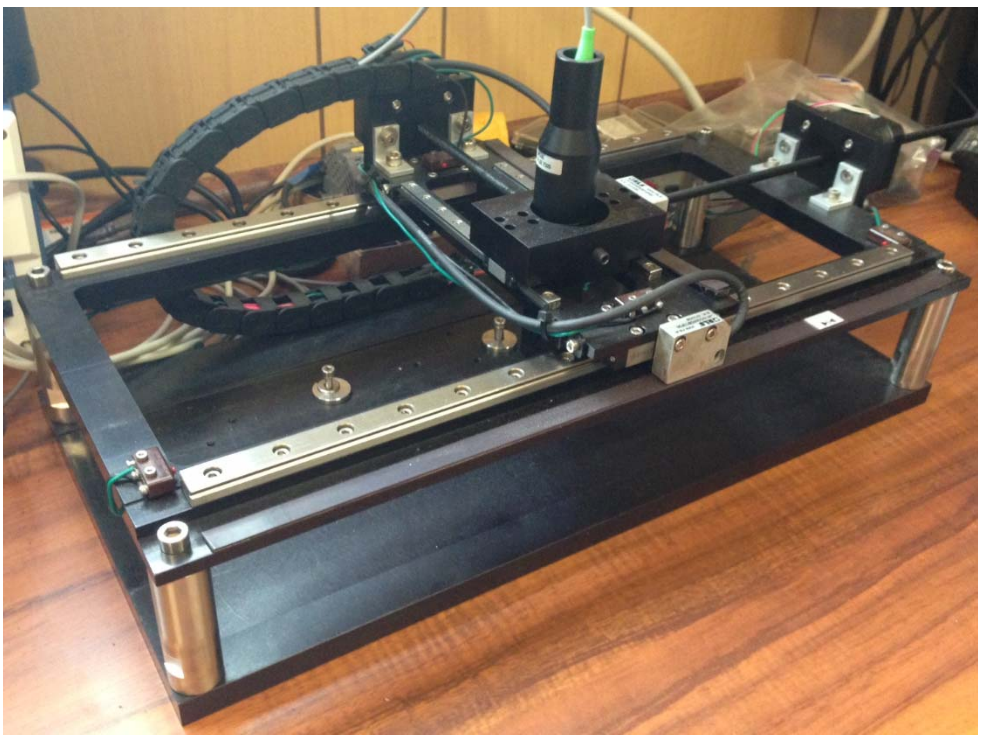

Figure 2-5: Photograph of Makai's motorized profilometer X-Y stage.

2.4. ULTRASONIC APPARATUS

The ultrasonic apparatus consists of a handheld flaw detector instrument and a motorized scanner. The Raptor® imaging flaw detector and the TunnelScan® are manufactured by NDT Systems Inc. The transducer is a D11 high resolution delay line type with a 0.250 inch element that operates at a frequency of 15 MHz. The suction cup feet of the ultrasonic scanner were removed and the assembly was mounted vertically on the back of the corrosion rack. The transducer is held pressed against the sample's surface by a spring loaded yoke on the X-Y scanner. Pressurized water is supplied to the transducer head to maintain a liquid interface with the sample. The Aluminum corrosion sample was scanned with a resolution of 0.001" x 0.001" daily. The measured thickness was plotted with software provided with the ultrasonic equipment.

(a) ***(b)***

Figure 2-6: (a) NDT Systems RAPTOR imaging flaw detector and (b) TunnelScan mounted on the back side of Makai's corrosion rack.

Figure 2-7: Front of the corrosion rack showing the aluminum sample through the acrylic glass. The ultrasonic apparatus can also be seen behind the sample.

3. VERIFICATION TEST

3.1. VERIFICATION SAMPLE

A test was performed to verify the correct operation of the integrated time-lapse and ultrasonic corrosion apparatus. A machined aluminum alloy 2024 plate measuring 1199 x 102 x 9.5 mm was used for the test. Because the ultrasonic scanner has a limited range of motion and has slow scanning speed, a 64 x 64 mm area at the center of the sample was chosen to be the representative test region. This 64 x 64 mm area of interest required one hour to scan with the ultrasonic apparatus at 0.5 mm resolution. At the corners of the area of interest, five 1.6 mm diameter holes were made to allow the imaging, ultrasonic and profilometery data to be indexed and referenced to each other. These holes were covered with epoxy resin such that they would not corrode and remain recognizable throughout the life of the test. A square area of the sample was also covered with a thin 0.1 mm layer of epoxy resin. This area of epoxy would not corrode and acted as a reference surface for the ultrasonic measurements. The profilometer was used to measure the actual hole diameters and depths of the manufactured calibration block.

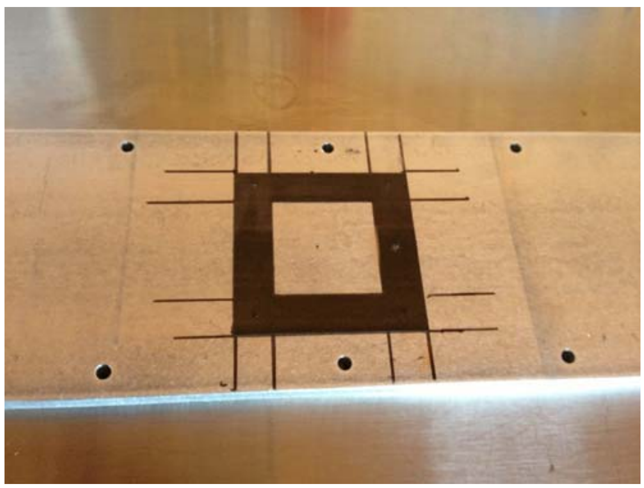

Figure 3-1: Photograph of the aluminum sample's center section showing the area of interest within the black epoxy square. The 5 holes were drilled in a square pattern and the region surrounding the area of interest was covered with a thin 0.1 mm layer of epoxy.

3.2. PROFILOMETRY SCAN

The area of interest on the aluminum sample's surface was scanned using the profilometer apparatus before epoxy coating and is shown in Figure 3-1.

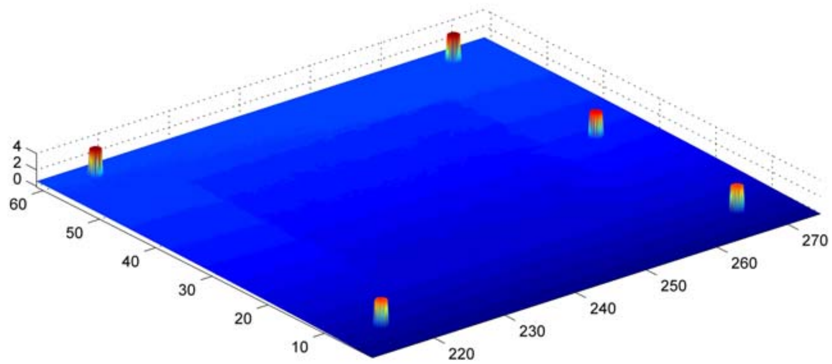

Figure 3-2: Isometric view of the profilometer scan data for the area of interest on the front side of ultrasonic coupon before epoxy application.

The optical profilometer scan of the aluminum corrosion sample before exposure to sea water revealed the true depth and dimensions of the indexing holes

3.3. IMAGING SCANS

The entire aluminum sample was scanned using the imaging apparatus on the first day of the test and the area of interested is shown in Figure 3-1. No corrosion of the aluminum sample was visible in this first scan.

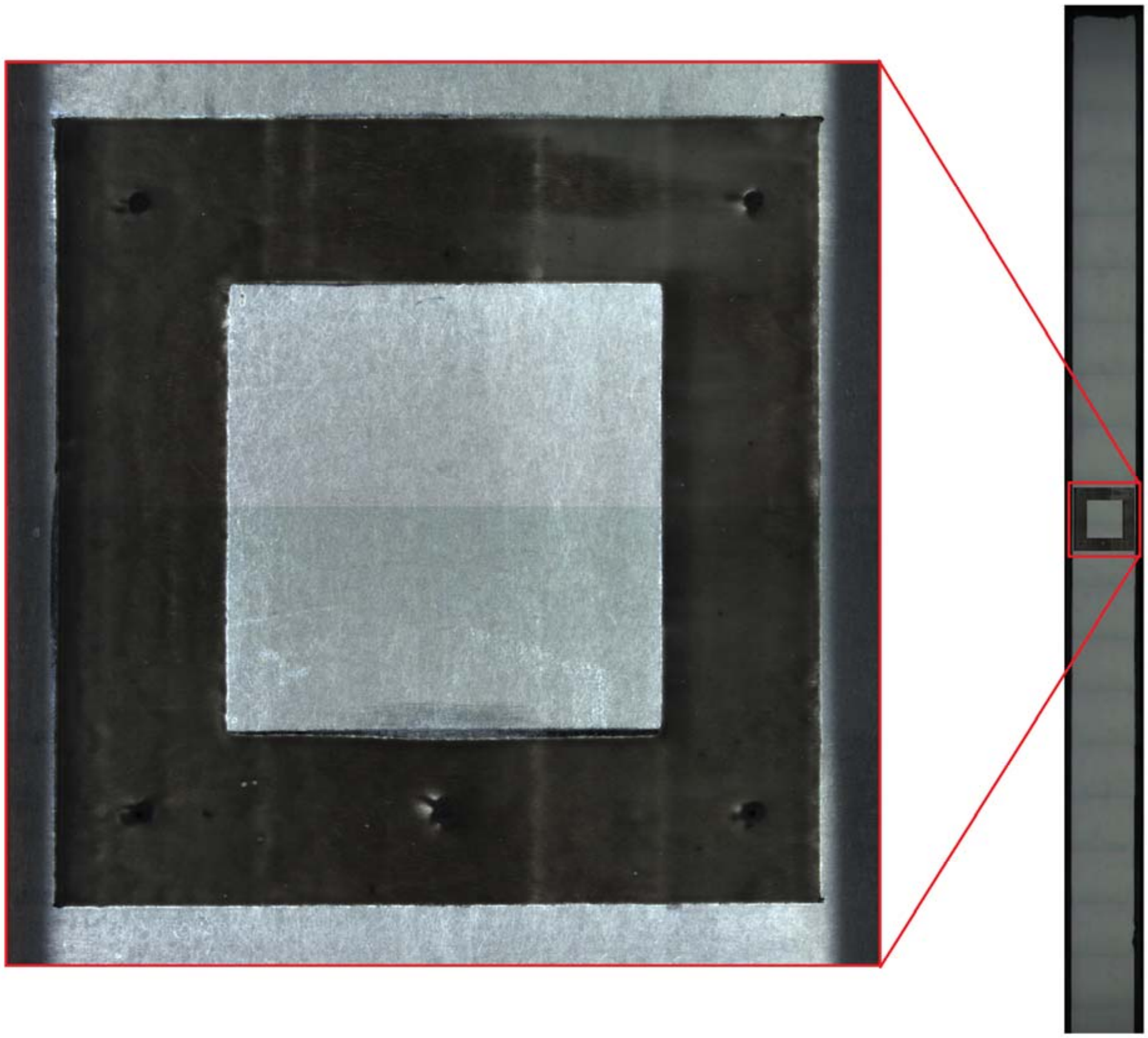

Figure 3-3: Photograph of the front of the aluminum sample. The zoomed in image shows the area of interest that was scanned by the profilometer and ultrasonic apparatus. The five holes can be seen as black dots. The black area is the thin 0.1 mm layer of epoxy that was applied to the surface after the holes were made.

3.4. ULTRASONIC SCANS

The thickness of the sample's area of interest was scanned on the first day of the test using the ultrasonic apparatus with a resolution of 0.005 x 0.005 inches and is shown in Figure 3-2. The five indexing holes were identified in the ultrasonic scan. The initial thickness of the plate was determined to be 0.375in.

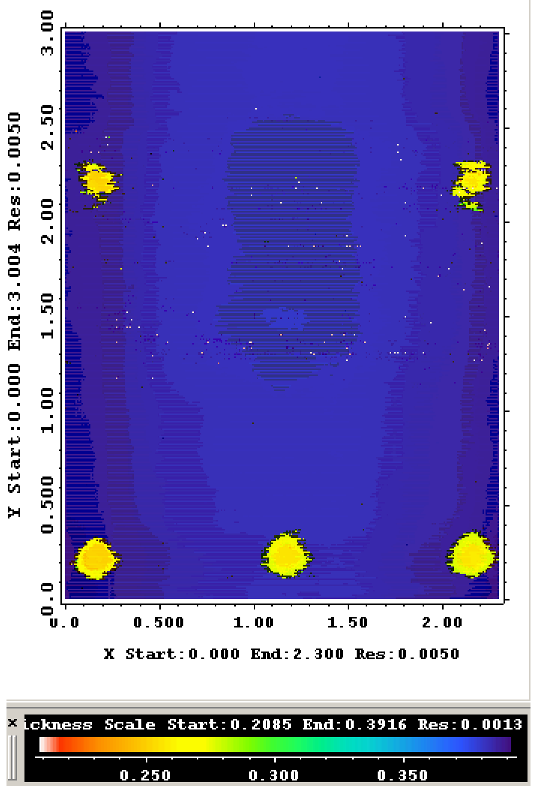

Figure 3-4: The material thickness of the aluminum sample's area of interest. The scan was performed at a resolution of 0.005"x0.005" on the back side of the aluminum sample. The indexing holes can be seen as yellow circles in the thickness plot.

4. CONCLUSIONS AND DISCUSSION

4.1. IMAGING APPARATUS

The imaging apparatus was designed, fabricated and assembled as planned without any major modifications. The precise encoders allow the images to be accurately stitched together. The image quality is excellent. The software was developed such that the daily sample imaging is automated. This daily imaging will allow us to produce a time-lapse sequence of images showing pitting corrosion progress through time.

4.2. ULTRASONIC APPARATUS

The ultrasonic apparatus purchased from NDT Systems was rigidly mounted on the back of the corrosion rack without any major modifications. The stainless steel framed transducer had to be slightly offset from the sample surface as not to scratch the soft aluminum. A continuous water supply had to be provided to the transducer holder to maintain liquid between the transducer and the sample. The pressured water vessel that was purchased with the NDT TunnelScan was too small and ran out of water before the scan was completed. The problem was solved by adding a pressurized fresh city water line to the transducer head. The ultrasonic apparatus was able to successfully measure the aluminum sample's thickness and detect the indexing holes. During the corrosion test the sample will be scanned every day. At the end of the test the ultrasonic data will be analyzed to determine the rate of pit growth and deepening.

OTEC HEAT EXCHANGER PROGRAM

PROGRESS REPORT #4

Prepared For

HAWAII NATIONAL MARINE RENEWABLE ENERGY CENTER

LUIS VEGA

1680 East West Road, POST 112A

Honolulu, HI, 96822

USA

Prepared By

MAKAI OCEAN ENGINEERING

PO Box 1206, Kailua, Hawaii 96734

August, 2013

SUMMARY

A detailed procedure for in-situ measuring of pitting corrosion in aluminum alloys has been developed. Makai has applied its experience from continuing corrosion research to develop this procedure which includes: sample preparation, installation, data collection, sample processing, and data analysis. This method combines photographic imaging, ultrasonic inspection, and laser profilometry to provide an encompassing picture of the pitting phenomena. The comparison of photographic imagery and ultrasonic data provides insight into pitting formation, growth and passivation rates. Ultrasonic inspection allows for the measurement of pit depth and the rate of deepening in-situ. The accuracy of these measurements is validated using the laser profilometer. This procedure serves as a guide to integrating these measuring techniques and is continuously evolving as new information is revealed.

1. INTRODUCTION

Aluminum corrodes in two ways: uniform corrosion and localized (pitting) corrosion. Uniform corrosion is a relatively slow reduction in metal distributed across the entire surface in contact with seawater, much like one sees on a rusting steel plate exposed to a mild marine environment. Pitting corrosion, in contrast, is an unpredictable, sudden and rapid attack of the metal at a single point on its surface. Pitting corrosion essentially ‘drills’ a hole in the metal at a rate of up to .002” per day. If the pit passes through the 1/8 inches wall of an OTEC heat exchanger, it would be a catastrophic failure. Our objective in this study is to develop a new technique for measuring pitting growth rates in order to better understand the differences between various alloys and manufacturing processes. Makai has developed several ideas for accurately measuring the growth of pits in situ, which will allow us to take multiple measurements of a single sample without removing it from the test rack. In addition, Makai wants to automate the process in order to reduce human error and allow for a much larger test. For example, counting individual microscopic pits manually is a very tedious process which is better suited to a computer. The initial method which Makai implemented and tested was photographic imaging. The second method which Makai wants to implement and test is ultrasonic imaging. Corrosion mapping, which is based on ultrasonic technology, is one technique used by industry to monitor wall thickness in piping or tanks. This technique utilizes the speed of sound travelling through a metal wall to determine its thickness. Typically, it is used as a safety precaution when hazardous materials are contained inside, especially if the pipe or tank is under pressure. Makai has confirmed this technique can be used to map the pits that develop in our aluminum samples. The benefit of this technology in our application is that we can monitor the growth of these pits, without removing the sample from the test. Once a pit is detected using the photographic imaging technique, the region will be scanned using an ultrasonic transducer. The change in thickness will be mapped according to its X-Y position using a motorized stage, and co-registered with the image data. Ultrasonic scans will be repeated on a daily basis to monitor changes. The main goal of the ultrasonic method is to determine the rate of pit growth through the wall, without removing the sample from the test rack. This information will be used to calculate the expected life of a heat exchanger.

2. PROCEDURE

2.1. SAMPLE PREPARATION

- Upon receipt, the samples are measured to verify dimensions are as designated on the drawings. Any difference in the sample thickness measured with the calipers compared with the ultrasonic flaw detector can be used to calibrate the ultrasonic flaw detector. This is done by adjusting the speed of sound setting on the flaw detector such that the two thickness measurements match.
- An area of interest is chosen to be the representative test region. At the corners of the area of interest, five 1.6 mm diameter holes are drilled to allow the imaging, ultrasonic, and profilometery data to be indexed and referenced to each other. The reference points will be referred to as fiducial points. These holes are covered with epoxy resin such that they do not corrode and remain recognizable throughout the life of the test. A square area of the sample is also covered with a thin 0.1 mm layer of epoxy resin. This area of epoxy will not corrode and acts as a reference surface for the ultrasonic measurements.
- Prior to exposure, samples are first degreased in a solution containing water and Simple Green, then rinsed with water, next rinsed with methanol, and finally allowed to air dry.

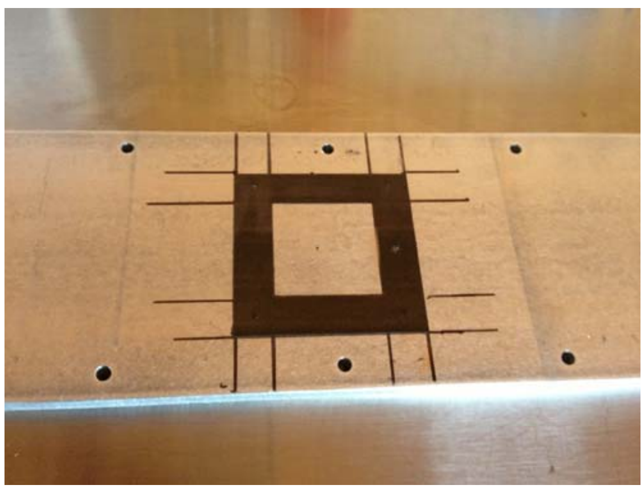

Figure 2-1: Photograph of the aluminum sample's center section showing the area of interest within the black epoxy square. The 5 holes were drilled in a square pattern and the region surrounding the area of interest was covered with a thin 0.1 mm layer of epoxy.

2.2. SAMPLE INSTALLATION

The samples are mounted to the back of the corrosion rack, allowing the front face to be exposed to flowing sea water. A gasket around the entire edge of the sample's front face seals the sea water channel.

Figure 2-2: Front of the corrosion rack showing the aluminum sample through the acrylic glass. The ultrasonic apparatus can also be seen behind the sample.

2.3. DATA COLLECTION

2.3.1. Imaging Scan

The entire sample including the area of interest is scanned using the imaging apparatus once a day. This scan takes twenty vertically tiled 5-megapixel color images of the sample with 10% overlap. The image resolution is 0.04 pixels per micron. An example of the overall daily image and a zoomed in view is shown in the follow figure.

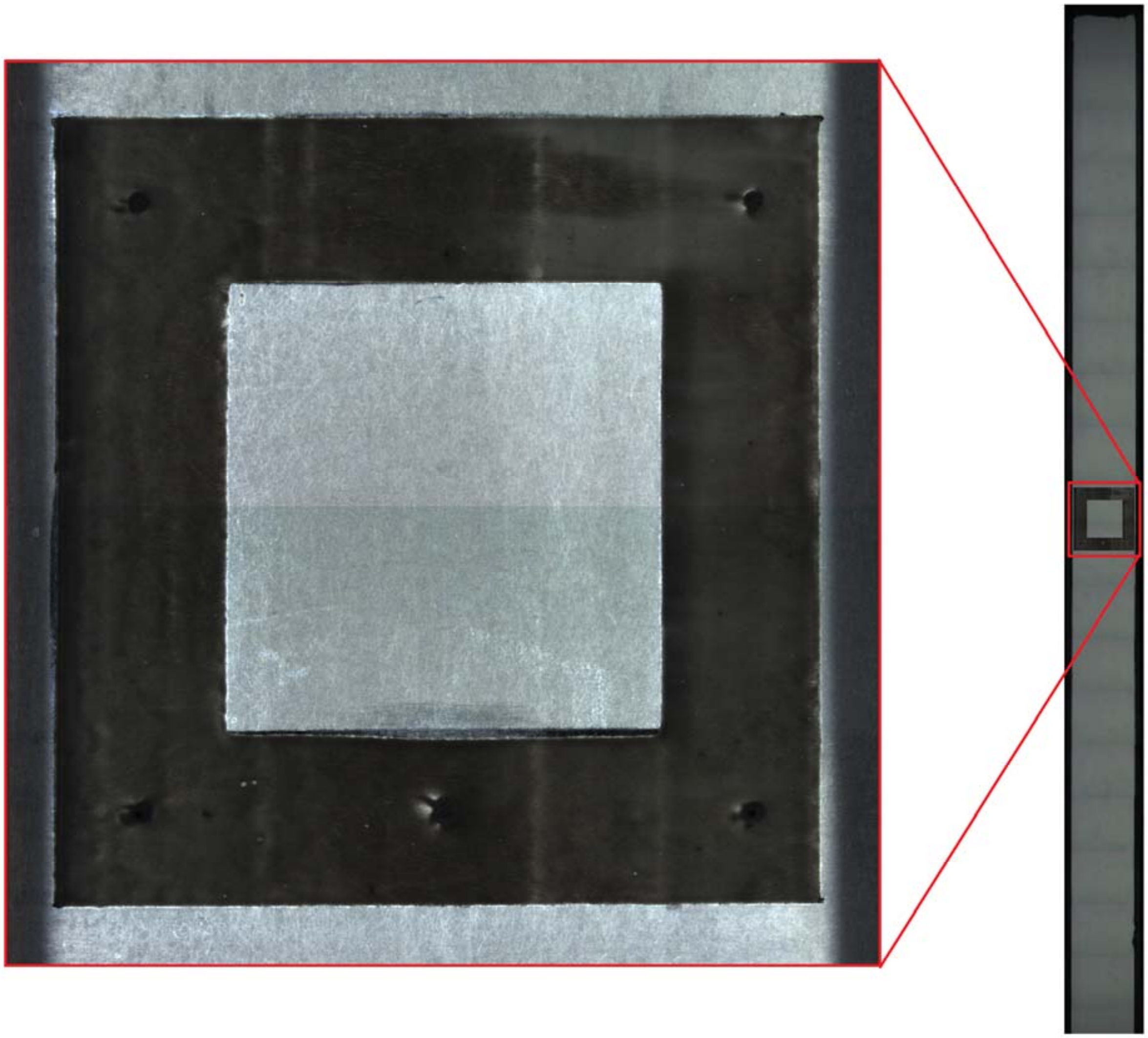

Figure 2-3: Photograph of the front of the aluminum sample. The zoomed in image shows the area of interest that was scanned by the profilometer and ultrasonic apparatus. The five holes can be seen as black dots. The black area is the thin 0.1 mm layer of epoxy that was applied to the surface after the holes were made.

2.3.2. Ultrasonic Scan

The ultrasonic apparatus is used to scan the sample's thickness profile in the area of interest. The transducer is mounted such that it is pressed against the sample's back surface with a spring loaded yoke. Pressurized water is supplied to the transducer head to maintain a liquid interface with the sample. The Aluminum corrosion sample was scanned with a resolution of 0.002" x 0.002" daily. Each scan line was scanned twice before moving to the next scan line. The data from the two lines were averaged and this helped to reduce noise in the data. The ultrasonic data can be plotted as a color map as in the example shown in the figure below.

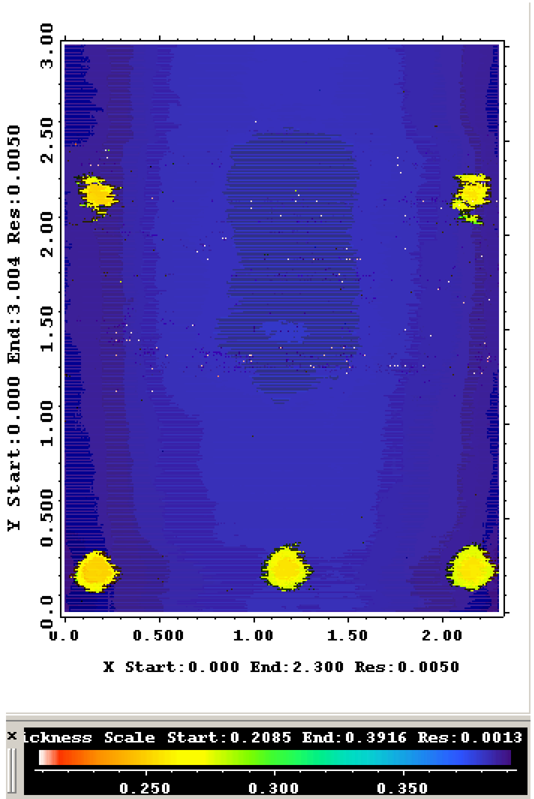

Figure 2-4: The material thickness of the aluminum sample's area of interest. The scan was performed at a resolution of 0.005"x0.005" (units in inches) on the back side of the aluminum sample. The indexing holes can be seen as yellow circles in the thickness plot.

2.3.3. Profilometer Scan

The profilometer scan is conducted on the sample's frontal corroded surface after removal and post-processing (section 2.4). The sample is clamped to the profilometer stage and the surface is wiped with a methanol wetted lint free cloth. Clean compressed air is blown on the sample to remove any loose particles on the surface or in the corrosion pits. The LED setting of the profilometer is set such that the intensity is within range (2.0 - 99.8%) while measuring both the un-corroded and corroded surface areas of the sample. The data acquisition rate is set to 1000Hz and the scan speed set to 100mm/second to achieve a desired spatial resolution of 0.1mm. An example of the profilometer data plotted in 3-D is shown in the following figure.

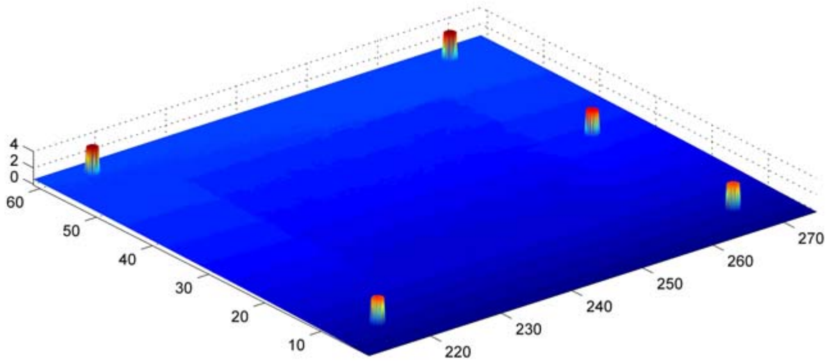

Figure 2-5: Isometric view of the profilometer scan data for the area of interest on the front side of ultrasonic coupon before epoxy application.

2.4. SAMPLE POST PROCESSING

- At the end of a test, the sample is removed from the corrosion rack and post-processed. Processing includes removing the epoxy and corrosion product so that the pitting corrosion can be imaged from the front using the profilometer. Sample removal requires stopping seawater flow and flushing the column with freshwater for a minimum of 5 minutes prior to opening the rack. This helps remove salt from the surface of the coupon so that it does not dry out with a layer of salt or sit in stagnant seawater.
- Once the flushing is complete, the sample is removed from the rack. The epoxy is removed by scrubbing the samples with a nylon brush while immersed in acetone. Finally, samples are immersed in a Nitric acid corrosion product removal bath (HNO3, sp gr 1.42) for 1-5 minutes or until all corrosion product is removed. The sample is then rinsed and air dried.

2.5. DATA PROCESSING

Prior to analysis, the data from the three different instruments (camera, ultrasonic, profilometer) must be co-registered. The data from each source will be overlayed so that the three properties of single or multiple points could be analyzed over time. Assembling and registering the data will be approached differently for each data set.

2.5.1. Photographic imagery mapping

The corrosion sample is imaged with twenty vertically tiled photographs. The first step is to stitch these images together to form a single image for the area of interest. This is achieved using a transformation matrix. The transformation matrix applies a translation, stretch and rotation to the images such that they align perfectly. The imaging system is indexed to the corrosion sample; leading to very consistent image positioning. For this reason the transformation matrix is determined once experimentally and then set for the remaining image sets.

2.5.2. Ultrasonic and profilometer data mapping

The ultrasonic and profilometer instruments are not indexed to the corrosion sample, and therefore every dataset has to be indexed separately. For this purpose, indexing holes were drilled into the corrosion sample as a square pattern around the area of interest to act as fiducial markers. The fiducial markers (drilled holes) were identified by applying a threshold to the thickness/depth data. After the threshold, a pattern recognition algorithm was applied to find circle patterns within a specific diameter range. This algorithm identifies the holes and provides the x-y coordinates of their respective centers. The center points of the circles become the fiducial markers and the four corners of a square that contains the relevant data. A transformation matrix is applied to correct for rotation and stretch. The data is then interpolated on to a uniform grid. All the data sets are placed on the same uniform grid to allow for streamlined analysis.

2.5.3. Co-registering between data types

The three data types have different resolutions so they are processed onto three different equally sized uniform grids. Transformation matrices are created to map between the different data types.

2.6. DATA ANALYSIS

2.6.1. Ultrasonic Analysis

The ultrasonic thickness data over time is analyzed to determined rate of pit deepening. The thickness of the sample on the first day minus the last day highlights areas of significant change in thickness, i.e. pitting. A threshold is applied to this data to distinguish significant thickness change. Unwanted noise is removed using a low pass filter. The particle analysis algorithm then counts the number of pits, determines the center location of the pit, the pitted area, average pit depth and maximum pit depth. The thickness of these pit locations is plotted over the time period of the test to reveal the rate of pit deepening. If the data shows predictable behavior, a trend line can be fitted and an equation constructed to predict future rates of pit deepening in the respective aluminum alloys.

2.6.2. Profilometer Analysis

The profilometer data at the end of the test period is analyzed for pit depth and size. This information is used to determine the accuracy of pit depth as determined in-situ by the ultrasonic instrument. Discretizing pits in profilometry data can be a challenging task because they can be irregular in shape and intertwined. A low pass filter is used to remove the pitted points that are less than three pixels wide. The particle analysis algorithm then counts the number of pits, determines the center location of the pits, the pitted area, average pit depth and maximum pit depth. Pits are known to appear larger than they actually are in the ultrasonic scan due to sound reflections. Using the profilometer data, a relationship between ultrasonically measured pit size and actual pit size can be established.

2.6.3. Imagery Analysis

The imagery data set is analyzed for contrasting black or white spots that could indicate pitting corrosion. A list of possible pits with their location, color and size is created using the particle analysis algorithm. This list of possible pits is compared with the list of actual pits indentified in the ultrasonic and profilometer data. The list of possible pits can then be divided into three separate lists; aggressive pits, passive pits, and false pits. Aggressive pits exhibit a rapid rate of deepening. The depth of passive pits increases at a slow or stationary rate. Faux pits are locations that appear to be pits in the photographic imagery but which there is no pit measured using the ultrasonic or profilometry instruments. For each category of pits, characteristic temporal color/intensity patterns are sought. These patterns are changes of color/intensity of image pixels over time. If these characteristic patterns can be established; they can be used in-situ for pitting prediction in current and future corrosion tests.

OTEC HEAT EXCHANGER PROGRAM

PROGRESS REPORT #5

Prepared For

HAWAII NATIONAL MARINE RENEWABLE ENERGY CENTER

LUIS VEGA

1680 East West Road, POST 112A

Honolulu, HI, 96822

USA

Prepared By

MAKAI OCEAN ENGINEERING

PO Box 1206, Kailua, Hawaii 96734

October, 2013

SUMMARY

Makai has performed a complete run through of their in-situ pit measurement test procedure. This method combines photographic imaging, ultrasonic inspection, and laser profilometry to provide an encompassing picture of the pitting phenomena. The comparison of photographic imagery and ultrasonic data provides insight into pitting formation, growth and passivation rates. Ultrasonic inspection allows for the measurement of pit depth and the rate of deepening in-situ. The accuracy of these measurements was compared to the final processed sample using a laser profilometer.

1. INTRODUCTION

Aluminum corrodes in two ways: uniform corrosion and localized (pitting) corrosion. Uniform corrosion is a relatively slow reduction in metal distributed across the entire surface in contact with seawater, much like one sees on a rusting steel plate exposed to a mild marine environment. Pitting corrosion, in contrast, is an unpredictable, sudden and rapid attack of the metal at a single point on its surface. Pitting corrosion essentially ‘drills’ a hole in the metal at a rate of up to .002” per day. If the pit passes through the 1/8 inches wall of an OTEC heat exchanger, it would be a catastrophic failure. Our objective in this study is to develop a new technique for measuring pitting growth rates in order to better understand the differences between various alloys and manufacturing processes. Makai has developed several ideas for accurately measuring the growth of pits in situ, which will allow us to take multiple measurements of a single sample without removing it from the test rack. In addition, Makai wants to automate the process in order to reduce human error and allow for a much larger test. For example, counting individual microscopic pits manually is a very tedious process which is better suited to a computer. The initial method which Makai implemented and tested was photographic imaging. The second method which Makai wants to implement and test is ultrasonic imaging. Corrosion mapping, which is based on ultrasonic technology, is one technique used by industry to monitor wall thickness in piping or tanks. This technique utilizes the speed of sound travelling through a metal wall to determine its thickness. Typically, it is used as a safety precaution when hazardous materials are contained inside, especially if the pipe or tank is under pressure. Makai has confirmed this technique can be used to map the pits that develop in our aluminum samples. The benefit of this technology in our application is that we can monitor the growth of these pits, without removing the sample from the test. Once a pit is detected using the photographic imaging technique, the region will be scanned using an ultrasonic transducer. The change in thickness will be mapped according to its X-Y position using a motorized stage, and co-registered with the image data. Ultrasonic scans will be repeated on a daily basis to monitor changes. The main goal of the ultrasonic method is to determine the rate of pit growth through the wall, without removing the sample from the test rack. This information will be used to calculate the expected life of a heat exchanger.

2. RESULTS

2.1. IMAGING SCAN

The entire sample including the area of interest was scanned using the imaging apparatus every day for 145 days. The images are viewed sequentially to observe the process of pitting corrosion. Nine representative photographs of the corrosion sample during the seawater submersion test are shown in the Figure 2-1. Day 0 shows the clean new aluminum surface immediately after submersion into seawater. On day 2 small black dots appeared on the surface. These were suspected of being pits. Two white circles of corrosion product were observed. By day 6 the sample surface had darkened and more dark colored circles became visible. Some of these dark circles were surrounded by a white contouring area. The sample continued to darken and acquire a reddish-copper hue by day 8. The dark circles clearly exhibited a contrasting white perimeter. Some clumps of white corrosion product were visible in areas of high pit density. At day 20 the sample color stabilized at dark copper. Some pits were visible as black dots surround by white corrosion product, while others were solely white shapes of corrosion product. Between days 20 and 77 very little change was noticed in the sample photographs except for slight increase in corrosion product in a few area. At day 99 the exposure time of the camera was increased to better illuminate the sample. Actual sample color did not change significantly from day 34 to day 99. Slight increase in white corrosion product was visible. At day 134 several large clumps of corrosion product were visible. By day 145 the while clumps of corrosion products had grown significantly. Several of these clumps had grown in size by a factor of two or more. Some small black circles were still visible although less discernable than earlier in the test.

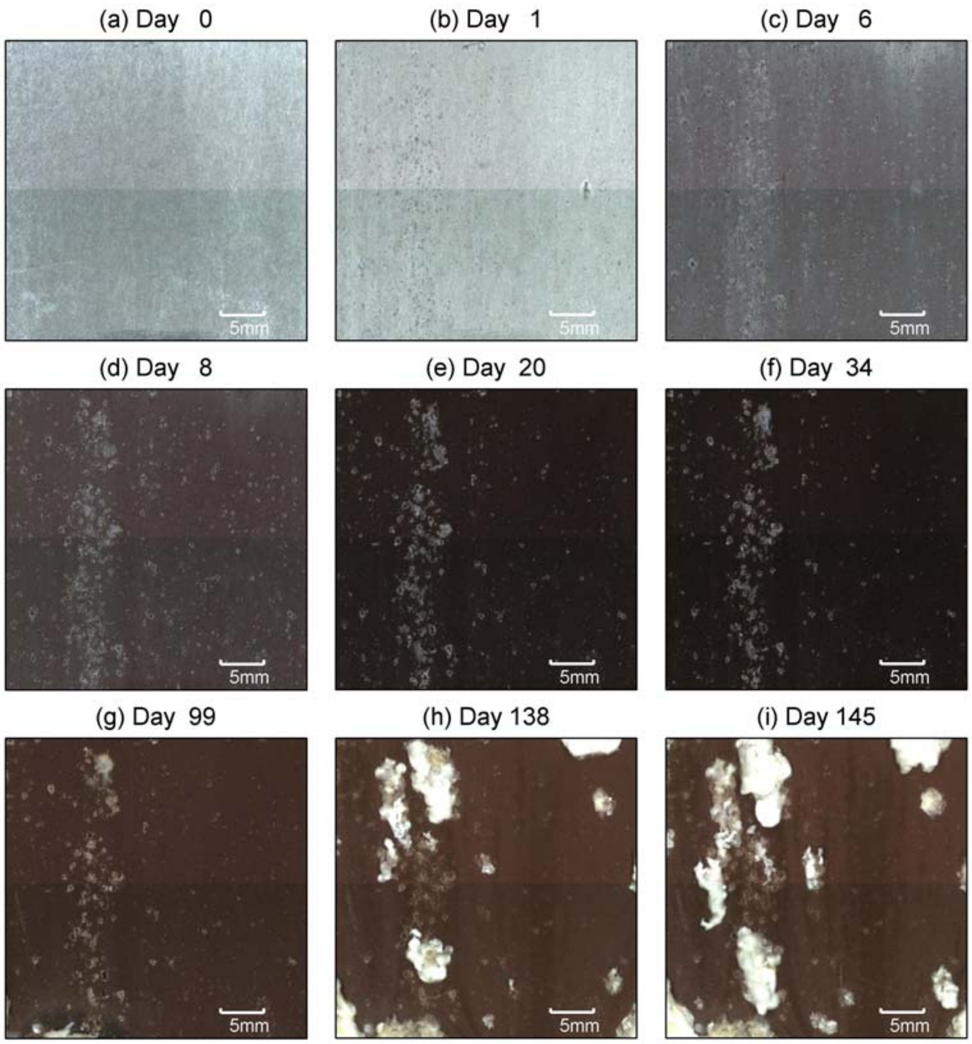

Figure 2-1: Front view photographs of the 2024 Aluminum sample's area of interest after indicated days of submersion in surface seawater. (a) Day 0; clean aluminum surface immediately after submersion. (b) Day 1; small pits are visible as black dots. (c) Day 6; sample surface has darkened and more dark colored pits with white surrounding corrosion product are visible. (d) Day 8; sample continues to darken and acquire a reddish hue. (e) Day 20; sample color stabilizes at dark copper. Some pits are visible as black dots surround by white corrosion product, while others are solely white shapes. (f) Day 34; not much change since day 20. Slight increase in corrosion product on largest pit visible at the top middle-left side of the photograph. (g) Day 99; exposure time of the camera was increased to better illuminate the sample. Actual sample color did not change significantly from day 34 to day 99. Slight increase in white corrosion product is visible. (h) Day 134; significant increase in white corrosion product in several areas since day 99. (i) Day 145; Increase in corrosion product is visible.

2.2. ULTRASONIC SCAN

The Aluminum corrosion sample's area of interest thickness profile was scanned at 14 intervals during the course of the 145 day test. Change in thickness was determined by subtracting the first day's thickness profile from the subsequent 13 thickness profiles.

2.2.1. Uniform Thickness Change

In the non-pitted area of the sample, there was a 0.065 mm average change in thickness between day 1 and day 145. This relatively uniform change in thickness could be attributed to the process of uniform corrosion, instrument drift or a combination of the two. In our hollow extrusion corrosion experiments we quantified uniform corrosion by precisely measuring the sample weight before and after seawater immersion. The average change in thickness for six different aluminum alloys was 0.010 mm over the course of 145 days. The large difference between the ultrasonically measured change in thickness for the 2024 sample and the six aluminum allows suggest possible instrument drift. Further investigation is required to determine the accuracy of this uniform change in thickness.

2.2.2. Localized Thickness Change

The change in thickness due to pitting corrosion (pit depth) was defined as the total change in thickness minus the uniform change in thickness. The pit depth over time is shown in Figure 2-2.

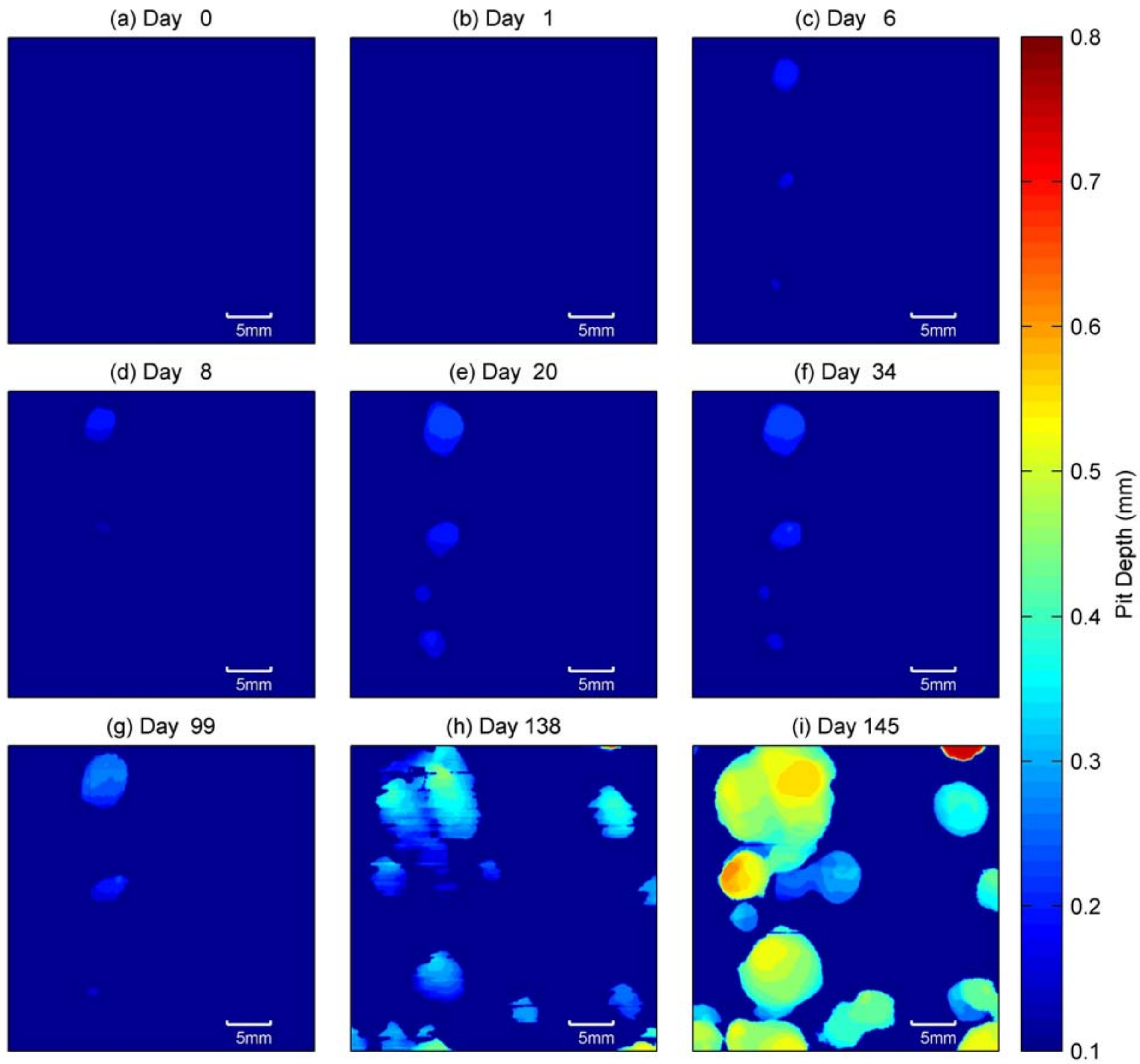

Figure 2-2: Ultrasonically measured depth of pitting corrosion in the 2024 Aluminum sample's area of interest after indicated days of submersion in surface seawater. The data was collected at a spatial resolution of 0.05mm x 0.05mm and filtered using an erode, dilate, and Gaussian blur to remove high frequency sensor noise.

Pits were identified and quantified using a threshold depth. Any group of adjacent points deeper than the threshold was considered a pit. Since pits come in many shapes and sizes, no shape detection was used. The threshold depth of 0.12 mm was set to be slightly larger than the irregularities in the surface. Pits were identified in each pit depth profile, recorded and tracked through the life of the test. If two pits merged, this new larger pit would maintain the same identification number as the deeper of the first two pits. The record would show the deeper pit as continuing to exist and the shallower pit and ceasing to exist. The rate of pit deepening and pit widening is shown in Figure 2-3 and Figure 2-4.

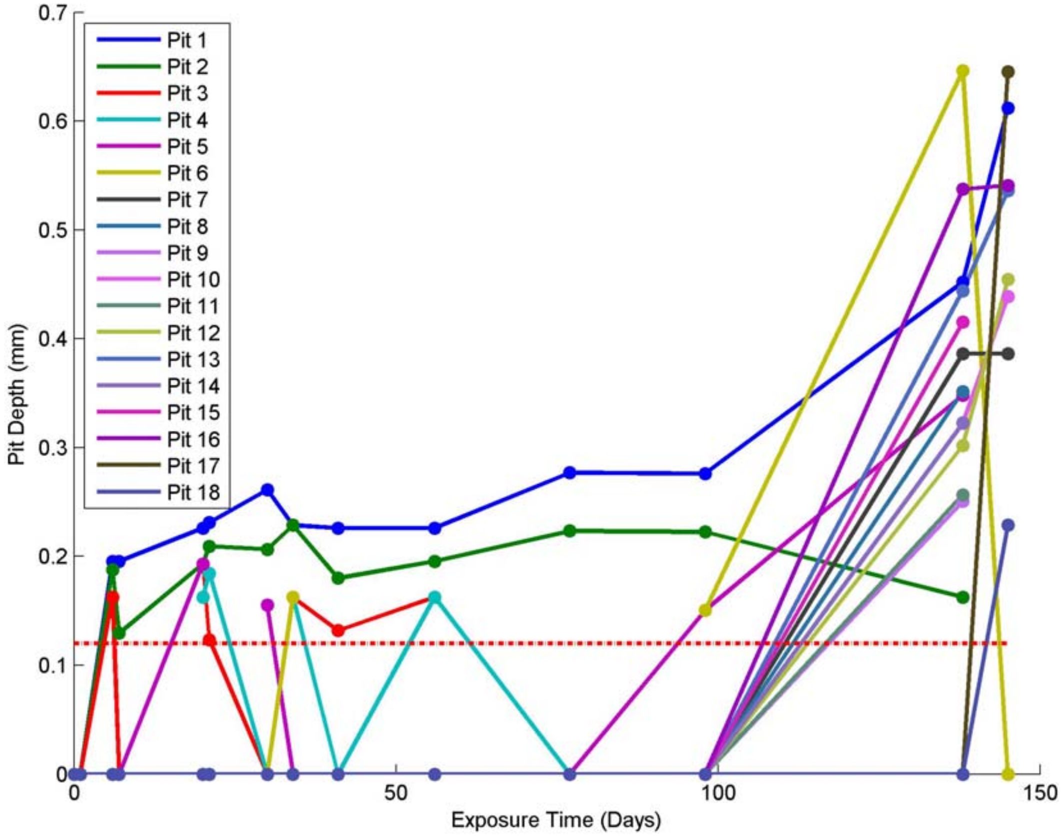

Figure 2-3: The ultrasonically measured depth of 18 tracked pits on the 2024 Aluminum sample submerged in surface seawater for 145 days. Pits were identified and quantified using a threshold depth of 0.12mm shown as the red dashed line. If a pit's depth was measured to be less than 0.12mm, it is shown as 0.0mm in this figure.

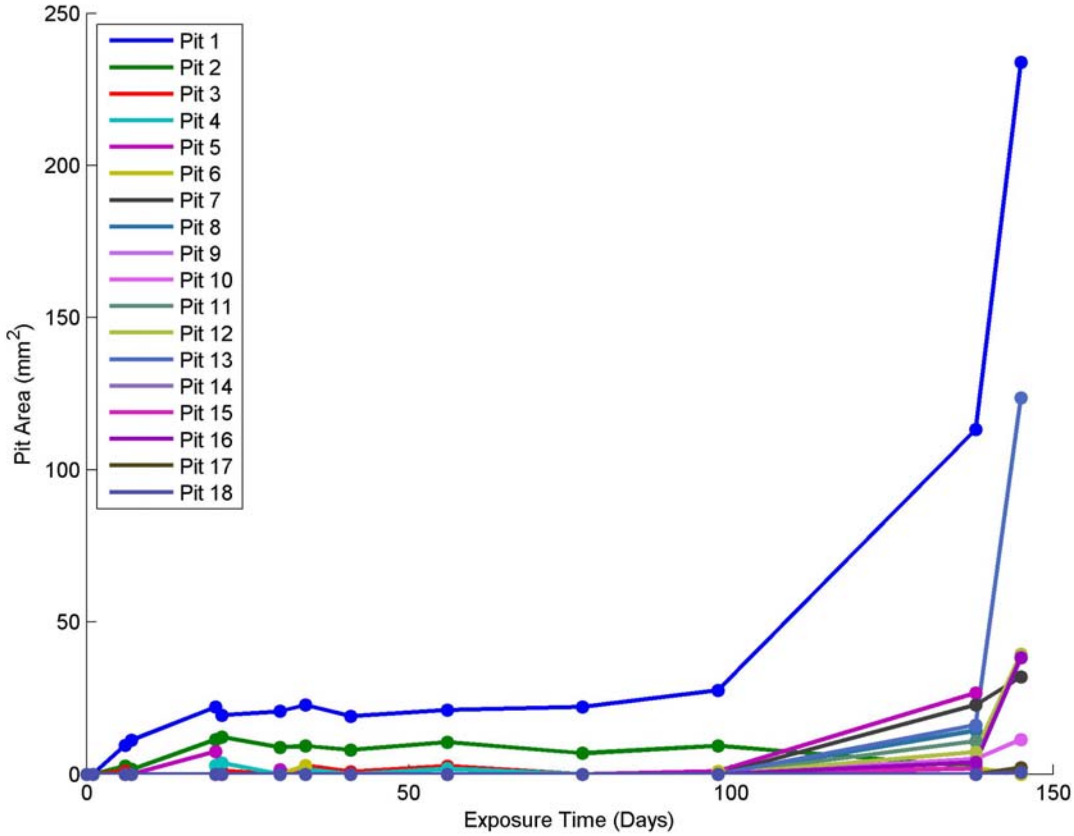

Figure 2-4: The ultrasonically measured area of 18 tracked pits on the 2024 Aluminum sample submerged in surface seawater for 145 days. Pits were identified and quantified using a threshold depth of 0.12mm. If two pits merged, this new larger pit would maintain the same identification number as the deeper of the first two pits. These pits can exhibit rapid increases in area when they merge with other pits. The shallower of the first two pits is no longer measured and its plotted line on the graph is terminated.

In this experiment the individual pits exhibited different behavior and must be discussed as separate groups. Pits 1 and 2 deepened quickly in the first week and then slowed to a much more gradual deepening rate. At approximately 100 days, pit 1 experienced another rapid deepening stage, while pit 2 became shallower and was consumed by another larger pit. Similarly, the pitted area of pits 1 and 2 grew rapidly in the first 20 days of exposure. At approximately 100 days, pit 1 began to grow rapidly while pit 2 became smaller and was consumed. Many new pits were identified on day 138. Many of these newly identified pits merged into fewer larger pits by day 145.

2.3. PROFILOMETER SCAN

At the end of the test on day 145 the sample was removed from the seawater rack. The post-processing procedure was applied to remove the corrosion product from the surface.

Figure 2-5: Photograph of the 2024 Aluminum sample's area of interest in air after 145 days of submersion in surface seawater, removal and post processing.

The sample's frontal corroded surface was scanned using the profilometer at a resolution of 0.1mm x 0.1mm.

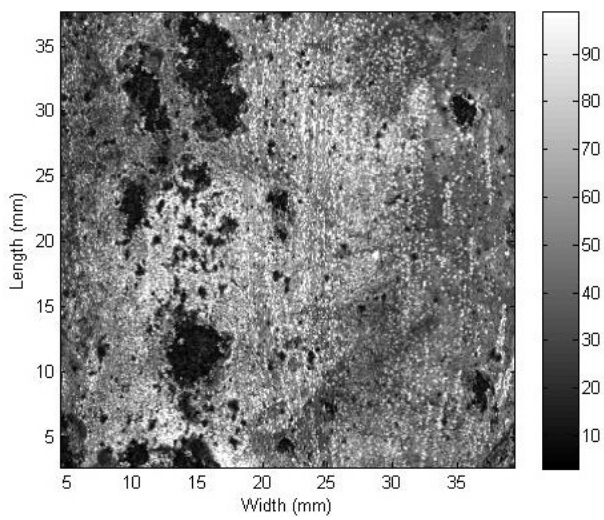

Figure 2-6: Intensity image of the 2024 Aluminum sample's area of interest after 145 days of submersion in surface seawater using the profilometer. The data was collected at a spatial resolution of 0.1mm x 0.1mm.

A filter was applied to the data to remove the best-fit-surface. The filtered profilometer depth is shown as a 3-D surface and as a color map in Figure 2-7. The profilometer shows several large deep pits and many small pits.

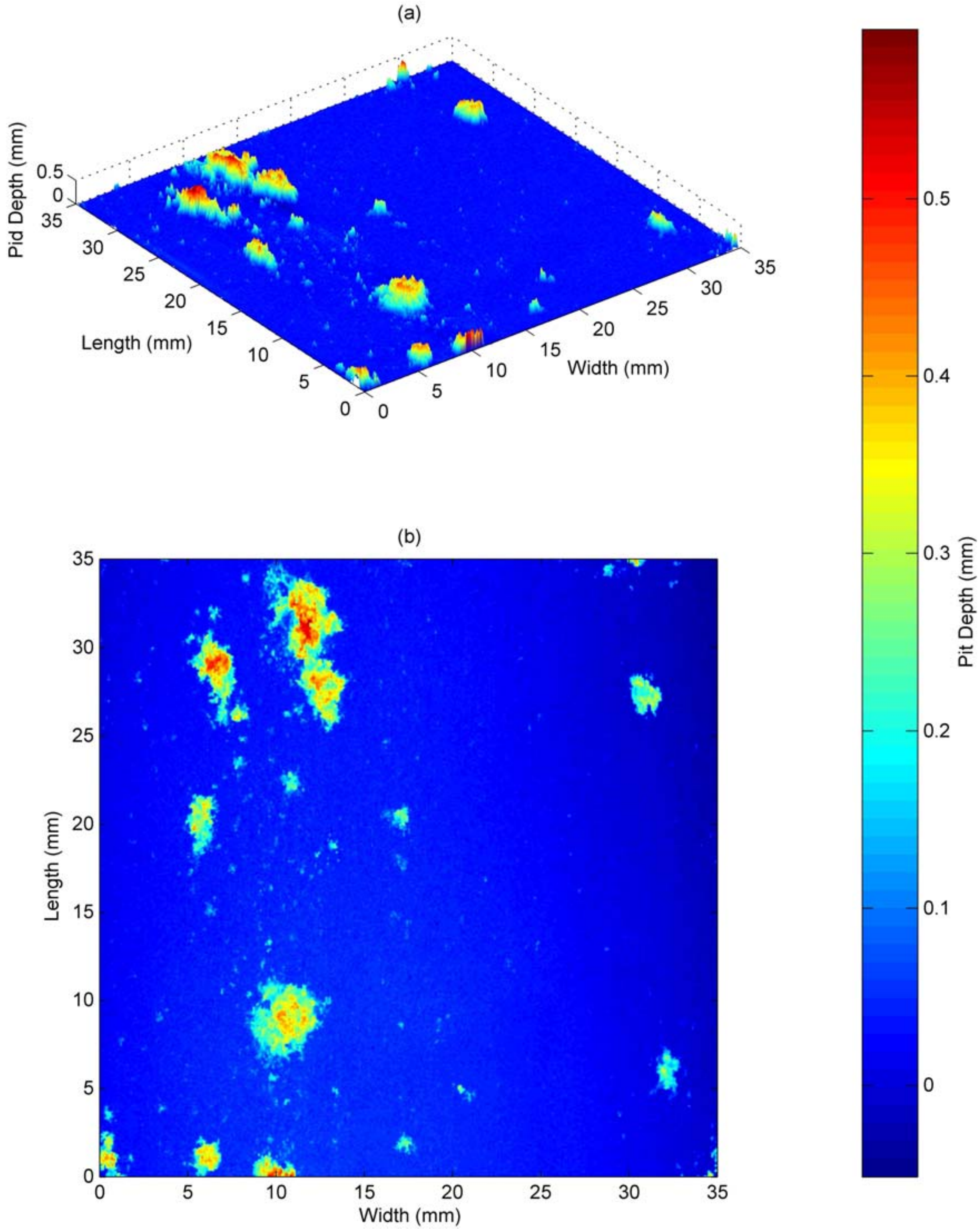

Figure 2-7: (a) Isometric and (b)Front view of profilometrically measured pit depth of the 2024 Aluminum sample's area of interest after 145 days of submersion in surface seawater. The pit depth in (a) is shown in the positive z direction for clarity. The data was collected at a spatial resolution of 0.1mm x 0.1mm. A second order polynomial filter was used to remove the best-fit-surface.

2.4. IMAGE WITH ULTRASONIC COMPARISON

The ultrasonic data was mapped and overlaid onto the photographic image data. A representative set of images with ultrasonically measured pit depth contours overlaid is shown in Figure 2-8. In the first 10 days many small dark circles form on the surface of the sample as seen in the photographs. During this time only 3 pits were detected with the ultrasonic flaw detector. The largest ultrasonically detected pit in the top left quadrant of the area of interest exhibited white corrosion product in the photographs. The other two ultrasonically detected pits did not exhibit significant corrosion product in the surrounding areas. The ultrasonically detected pits were found in an area with the highest visually perceived pit density. By day 99 a large clump of corrosion product remained over the largest and deepest ultrasonically detected pit. There was some corrosion product near the other ultrasonically detected pits, but not clearly correlated. At day 138 large clumps of white clumps of white corrosion product were visible over most of the ultrasonically detected pits except for one. By day 145 all the ultrasonically detected pits had visible white corrosion products over them. The deepest pits appeared to have the largest clumps of corrosion product over them.

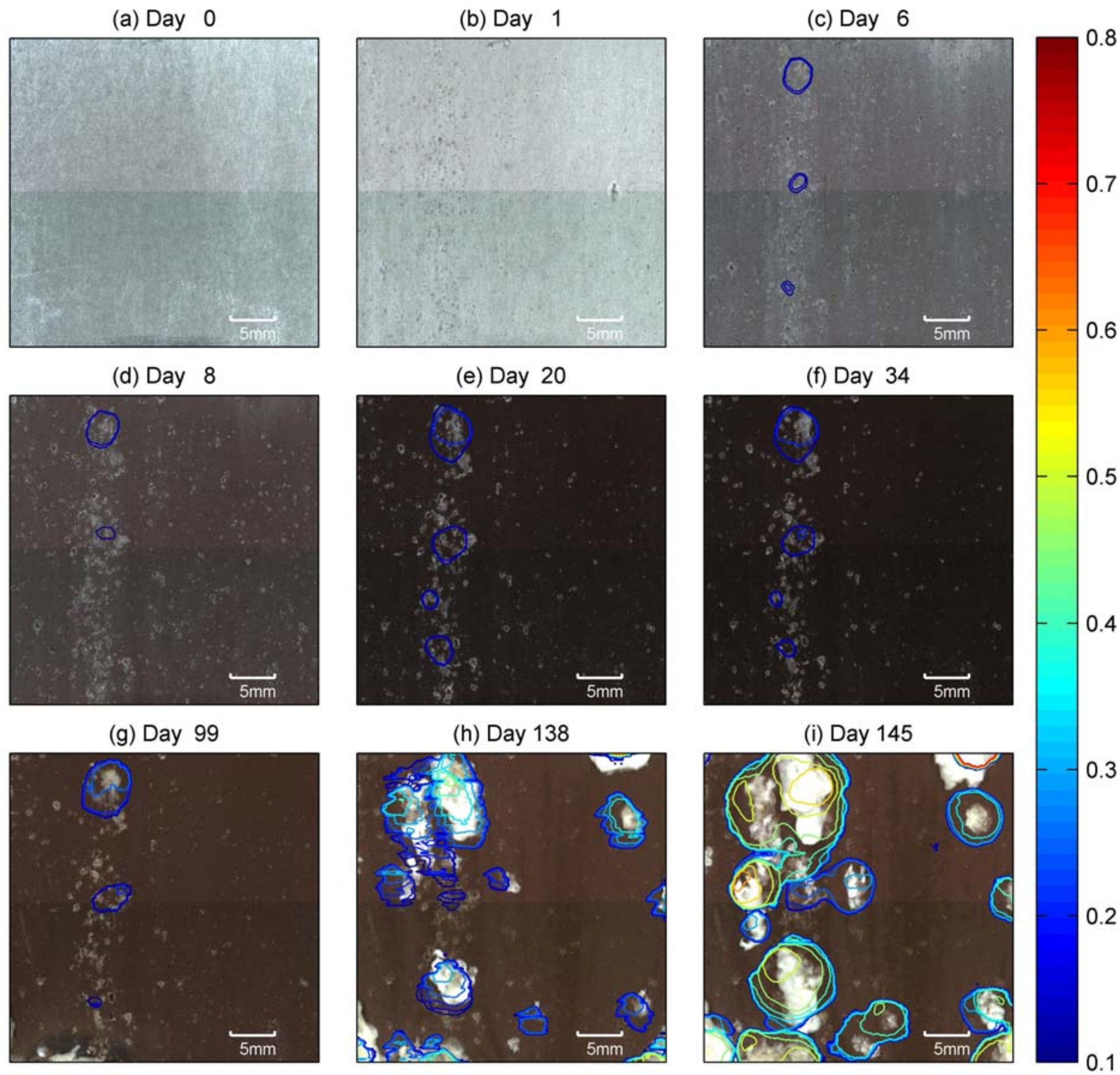

Figure 2-8: Front view photographs of the 2024 Aluminum sample's area of interest after indicated days of submersion in surface seawater with ultrasonically measured pit depth contours overlaid. (a) Day 1; no pits detected. (b) Day 6; three pits detected at 0.15mm deep. (c) Day 34; two pits deepen to 0.20mm and fourth 0.15 mm pit detected. (d) Day 99; deepest pit reaches depth of 0.45mm. Small increase in white corrosion product is visible over the deepest pit. (e) Day 138; many new pits detected and new large white corrosion product deposits visible. The visible white corrosion product correlates well with the ultrasonically detected pits. (f) Day 145; pits deepen and visible white corrosion product increases.

2.5. PROFILOMETERY WITH ULTRASONIC COMPARISON

The ultrasonic data from the last day was mapped and overlaid onto the profilometer data from the last day. A profilometer depth color map with ultrasonically measured pit depth contours overlaid is shown in the Figure 2-9 (a) below. Two cross sectional views of the depth data allow for comparison between the ultrasonic and profilometer measurements in Figure 2-9 (b) & (c). It can be seen from the color map and the cross sections that the ultrasonic instrument measured the pits slightly deeper and substantially wider than the profilometer. Thirteen pits identified in the profilometry data were associated with six pits in the ultrasonic data. In the ultrasonic data, pits appear wider than they actually are and overlap occurs. Figure 2-10 maps six pits that were identified in both data sets and their depths and areas were compared. The depth of the deepest pit within its cluster in the profilometer data is compared with its associated pit in the ultrasonic data. The area of all the pits in the cluster is summed and compared with its associated pit in the ultrasonic data.

Table 2-1 lists the measured depths, areas, and error in mm between the ultrasonic and profilometer measurements for these pits. The ultrasonic instrument measured the pits to be consistently deeper than the profilometer did as shown in Figure 2-11. Dimensional depth errors between the profilometer and ultrasonic instruments were between 0.05-0.33mm. Dimensional area errors between the profilometer and ultrasonic instruments were between 6.50 and 202.05 mm^2. The accuracy of the profilometer instrument is an order of magnitude higher than the ultrasonic (0.001 mm compared to 0.03 mm) and is generally used as the reference measurement. However, the profilometer is limited by line-of-sight measurement and would not be able to measure the depth of a horizontal cave-type pit. The presence of sub-surface corrosion could possibly explain some difference between the ultrasonic and profilometer measurements.

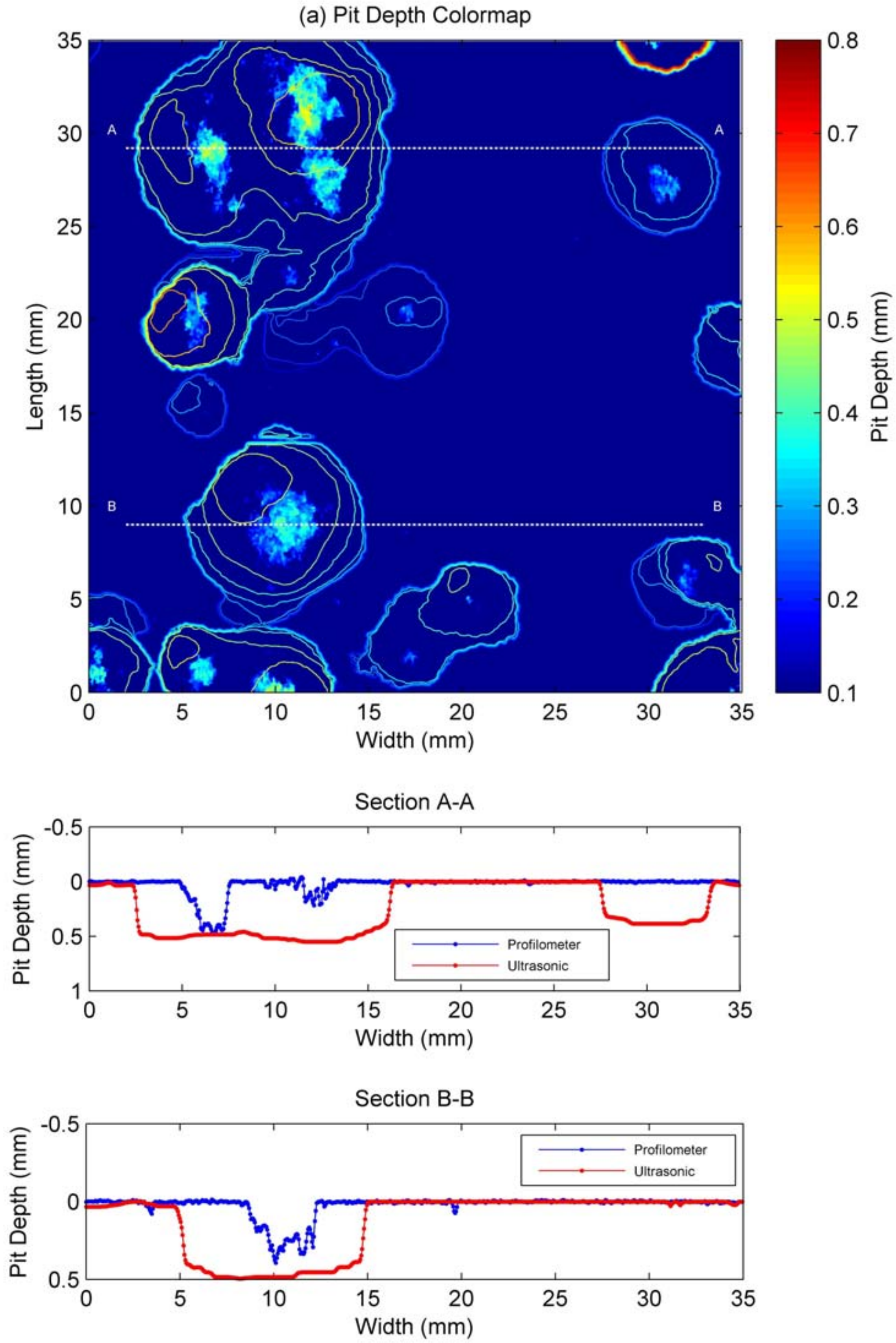

Figure 2-9: (a) Map of the 2024 Aluminum sample's area of interest after 145 days of submersion in surface seawater with profilometrically measured pit depth shown as a solid color, and ultrasonically measured pit depth contours overlaid. Both data sets use the color bar scale. (b)-(c) Cross section views showing depth data as measured with the profilometer (blue) and ultrasonic (red).

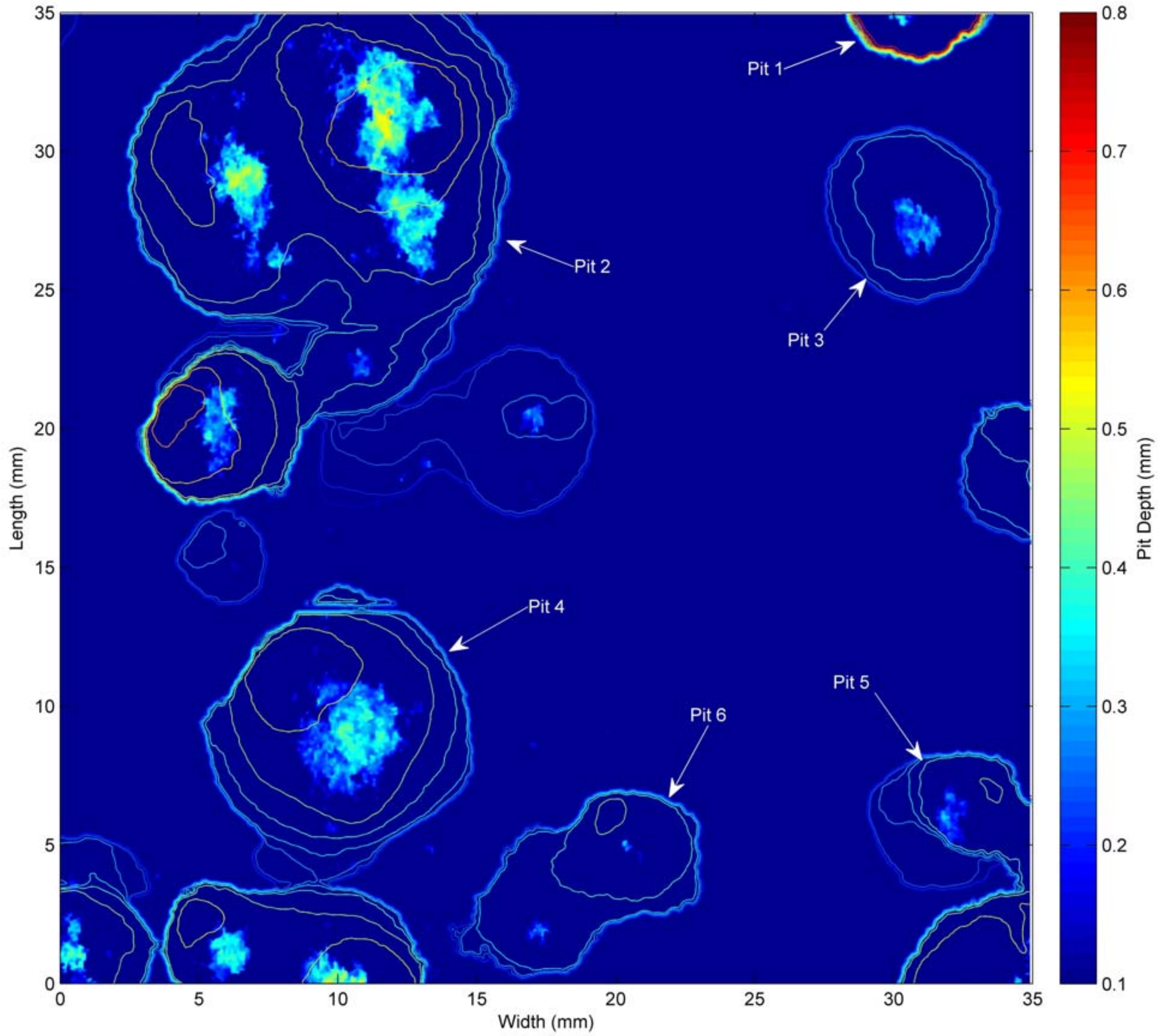

Figure 2-10 Map of the 2024 Aluminum sample's area of interest after 145 days of submersion in surface seawater with profilometrically measured pit depth shown as a solid color, and ultrasonically measured pit depth contours overlaid. Both data sets use the color bar scale. Six pits are identified and labeled for comparison between the ultrasonic and profilometer data.

Table 2-1: Comparison of pit depth and pitted area of the 2024 Aluminum sample's area of interest after 145 days of submersion in surface seawater measured using ultrasonic and profilometry techniques.

PIT	ULTRASONICALLY MEASURED SIZE (MM)		PROFILOMETER MEASURED SIZE (MM)		DIMENSIONAL ERROR (MM)	
TAG	DEPTH	AREA	DEPTH	AREA	DEPTH	AREA
1	0.74	7.30	0.41	0.79	0.33	6.50
2	0.61	233.94	0.47	31.89	0.14	202.05
3	0.39	31.95	0.34	3.28	0.05	28.67
4	0.54	123.73	0.43	18.44	0.10	105.29
5	0.54	38.30	0.32	2.02	0.22	36.29
6	0.45	39.50	0.24	0.48	0.22	39.02
		AVERAGE DIMENSION ERROR (MM)			0.18	69.64
		MAXIMUM DIMENSION ERROR (MM)			0.33	202.05

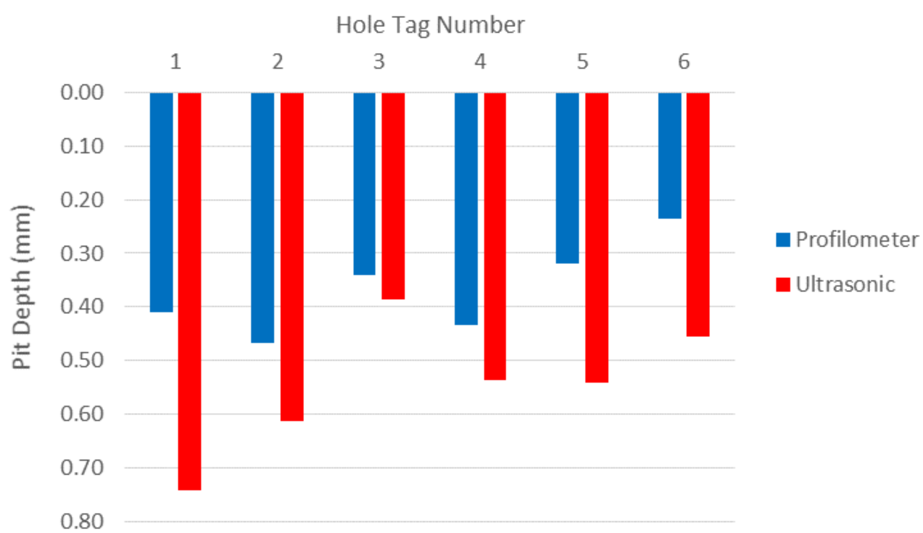

Figure 2-11: Comparison of pit depth of the 2024 Aluminum sample's area of interest after 145 days of submersion in surface seawater measured using ultrasonic and profilometry techniques.